МЕТОДИ КЕРУВАННЯ ТА ОЦІНЮВАННЯ В УМОВАХ НЕВИЗНАЧЕНОСТІ

UDC 629.7.05; 681.5.015

ELLIPSOIDAL ESTIMATION OF PARAMETERS OF ROTATIONAL AND TRANSLATIONAL MOTION OF A NON-COOPERATIVE SPACE VEHICLE FROM VISUAL INFORMATION

Nikolay Salnikov

Space Research Institute of NAS of Ukraine and SSA of Ukraine, Kyiv,
orcid: 0000-0001-9810-0963

salnikov.nikolai@gmail.com

Serhiy Melnychuk

Space Research Institute of NAS of Ukraine and SSA of Ukraine, Kyiv,
orcid: 0000-0002-6027-7613

sergvik@ukr.net

Vyacheslav Gubarev

Space Research Institute of NAS of Ukraine and SSA of Ukraine, Kyiv,
orcid: 0000-0001-6284-1866

v.f.gubarev@gmail.com

The use of near-Earth space is currently complicated by the presence of space debris objects in Earth's orbit, which include spent stages of launch vehicles, inoperative spacecraft, and other large and small objects associated with human activity in space. One of the elements of solving the problem of space debris is the docking and capture of an uncontrolled non-cooperative space object or spacecraft by a so-called on-orbit servicing spacecraft to carry out further actions to repair it, refuel or change its orbit. The situation is complicated by the fact that, under the influence of various factors, uncontrolled space objects are in a state of rotation. The parameters of the orbital motion of such objects are known quite accurately from measurements from the Earth. To carry out safe approach and docking, knowledge of the parameters of rotational motion, as well as the parameters of relative motion, is also required. The most general case of motion of a non-cooperative tumbling spacecraft located in an elliptical orbit is considered. It is assumed that the three-dimensional graphic model of such spacecraft is known. The servicing spacecraft (SSC) is equipped with a mono camera that takes pictures of the non-cooperative spacecraft (NSC). Based on a comparison of the characteristic features of photographs and images obtained using the graphical model, the computer vision system (CVS) determines the distance vector to the so-called graphical coordinate system, rigidly fixed on the NSC and the quaternion of its relative attitude. The specific type of CVS is not considered. It is assumed that the SSC carries out some maneuvers near the satellite. All parameters of the SSC angular motion are assumed to be known. This

work considers the most general case of the relative motion of SSC and NSC. Using quaternion calculus, all basic kinematic and dynamic equations are obtained. The measured parameters are not enough to ensure safe rendezvous and docking with the NSC. The stochastic characteristics of errors of the CVS measurement are not assumed to be known and, accordingly, are not used. Only their maximum values are specified for them. We consider the use of new dynamic set-membership filter using ellipsoids to solve the problem of determining the parameters of the relative motion of the NSC which is in free uncontrolled motion. The filter can be implemented under conditions of the limited computational capability available on onboard processors. The relative motion parameters include the distance vector between the centers of mass (c.m.) of the NSC and the SSC, the relative velocity vector, the quaternion of the orientation of the main axes of inertia of the satellite relative to the inertial coordinate system, the ratio of the moments of inertia of the satellite, the vector of the position of the NSC c.m. in the graphical coordinate system. The properties of the proposed algorithm are demonstrated using numerical simulation. The results obtained are expected to be used in the development, creation and testing of a navigation system for the rendezvous and docking of the SSC, developed by a group of Ukrainian space industry enterprises under the leadership of the LLC «Kurs-orbital» (https://kursorbital.com/).

Keywords: relative motion parameters, spacecraft, estimation, video image.

Introduction

The presence of space objects related to space debris in near-Earth space poses a serious threat during the launch of spacecraft (SC), as well as for those spacecraft that are already in orbit. Some of these objects are inoperative spacecraft, which, with minor repairs or after refueling, can continue to operate. Therefore, work is currently underway all over the world to create so-called servicing spacecraft (SSC) or on-orbit servicing spacecraft capable of docking with a non-cooperating spacecraft (NSC) or object and performing maintenance or removing the object from orbit. The development and current state of this problem can be found in the reviews [1–4].

Success in docking significantly depends on the accuracy of determining the relative navigation of the NSC and SSC [5–7]. It is assumed that the navigation and attitude control systems of the NSC does not work for some reason. In this case, radar and optical systems are used to determine the relative position and attitude of the NSC. The latter include laser [8–12] and optical systems [13–30], which use cameras operating in the optical range. Optical systems are capable of providing more accurate measurements of the parameters of the relative position and attitude of the NSC at close distances (no more than 100 m) and are used at the final stage of docking. These devices allow to obtain values of the distance vector and the attitude of a certain reference frame rigidly fixed to the NSC. This information is not enough for trajectory planning and docking with the NSC. It was established [31] that the NSC eventually begins to rotate around the center of mass. This occurs due to the action of the gravitational moment, cosmic radiation and the flow of solar wind particles [32, 33]. For docking, it is necessary to know the position time evolution of the docking surface, which requires knowledge of the angular velocity of rotation of the NSC, the speed of approach, as well as the position of the main axes of inertia, the position of the center of mass. Currently, there are a large number of works devoted to solving the problem of estimating these parameters [8–17, 20–29, 34–36]. These works rely on the use of various versions of the Kalman filter [37–39] to estimate these parameters.

The Kalman filter and its many modifications use the assumption that the uncertain quantities are normally distributed random quantities. The distribution parameters are assumed to be known. However, determining these parameters is a separate, rather labor-intensive task. For more than half a century, a different approach [40–46] has been developing to the problem of estimating unknown quantities, in particular, estimating

the state vector of dynamic systems, which is based on the use of minimal information about uncertain quantities, namely, only the sets of their possible values are assumed to be known. As a result, the estimation process is reduced to procedures for calculating the evolution of sets and set-theoretic operations on them, i.e. to the construction of refined sets or, as they are commonly called, information sets that are guaranteed to contain the estimated values. This approach is accordingly called guaranteed or set-theoretic. In most cases, the construction of information sets is associated with serious computational difficulties, which is an obstacle to their practical implementation, in particular, with the help of on-board computer systems. The use of the ellipsoidal estimation method [40, 42–46] seems to be quite effective in terms of functionality and minimization of computational costs, including state estimation of nonlinear dynamic systems [47–51]. In accordance with this method, information sets are approximated by multidimensional ellipsoids. The ellipsoidal estimation method is sensitive to violations of a priori assumptions about the values of uncertain quantities. To overcome this disadvantage, i.e. to ensure the robustness property, several modifications of this method have been proposed [52–55].

The purpose of the work is to study and develop an algorithm for solving the estimation problem of parameters of the angular motion of the NSC (attitude quaternion, angular velocity vector, ratio of moments of inertia, position of the main axes of inertia, position of the center of mass), vectors of the relative distance and speed between the SSC and the NSC based on a modification of the ellipsoidal estimation method [54, 55]. Any of the optical relative navigation devices mentioned above can be considered as an CVS device. The authors of this work focused on the use of CVS using a monocamera, which operating principle and algorithms are described in [26, 30]. The proposed estimation algorithms use the multiplicative form of quaternion increments [56, 57], which not only simplifies the quaternion normalization procedure compared to using the additive form of the increment, but also leads to simpler equations describing the dynamics of changes in quaternion increments. This work is a development of [58], and in terms of the formulation of the problem it is very close to [35].

1. Estimation problem statement

1.1. Coordinate systems. The position of SSC and NSC in space will be specified in the inertial geocentric equatorial coordinate system $O_E I = O_E i_1 i_2 i_3$, the origin of which is in the Earth center of mass (c.m.), the basis vector i_3 is directed along the Earth rotation axis, the vector i_1 is orthogonal to the vector i_3 and directed to the infinitely distant point of the vernal equinox. The direction i_2 is chosen in such a way that the triple of vectors i_1, i_2 and i_3 to be right-handed [59, p. 448]. Here and below, only orthonormal right-handed systems of basis vectors are considered. We will call this system in short the inertial reference frame (IRF).

The position of the SSC c.m. will be specified relative to the NSC c.m. The choice of the NSC as a reference object is due to the fact that the satellite's orbit is assumed to be known, the satellite does not perform any maneuvers, and the position of the satellite in orbit is known. The position of the NSC orbital plane relative to the IRF is characterized by the orbit inclination angle i, and the longitude angle Ω of the orbit ascending node relative to the axis $O_E i_1$ (see Fig. 1). The position of the NSC orbit in its plane is characterized by the angle $\bar{\omega}$ measured from the ascending node direction to the orbit perigee direction [59].

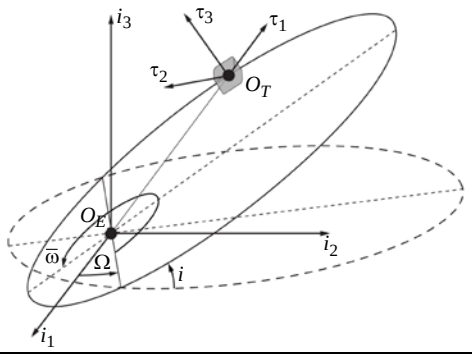

Fig. 1

The SSC position relative to the NSC will be characterized in the orbital reference frame (ORF) [59, p. 675] $O_T T = O_T \tau_1 \tau_2 \tau_3$, the beginning of which O_T is placed in the NSC c.m., the basis vector τ_1 is directed along the radius vector from the Earth c.m. to the NSC c.m., the vector τ_3 is perpendicular to the orbital plane and directed along the angular momentum vector of the NSC orbital motion, the direction of the vector τ_2 is chosen in such a way the triple of vectors τ_1, τ_2 and τ_3 to be right-handed (at circular orbit, the direction of τ_2 will coincide with the satellite's velocity direction).

Two more reference frames are associated with the NSC. Coordinate system $O_T e_1 e_2 e_3 = O_T E$, the center of which is located in the NSC c.m., and the unit vectors are oriented along the main axes of the NSC inertia tensor. This reference frame $O_T E$ will be further denoted by target reference frame (TRF). The so-called graphical coordinate system $O_G e_1' e_2' e_3' = O_G E'$ is also associated with the NSC, which we will briefly denote as Graphic reference frame (GRF). The satellite graphical model is specified in this coordinate system, and the coordinates of all elements of the satellite are specified, in particular, the position of the docking surface. The position of this coordinate system is determined by the computer vision system (CVS).

Coordinate system $O_C s_1 s_2 s_3 = O_C S$, which center O_C is located in the SSC c.m., and which unit vectors are oriented along the main axes of the SSC inertia tensor, characterizes the SSC attitude. This reference frame will be denoted as chaser reference frame (CRF). The coordinate system $O_V s_1' s_2' s_3' = O_V S'$ is associated with the CVS camera installed on the SSC. In this definition, O_V is the origin of the coordinate system, and s_j', $j = 1:3$ are the vectors of the orthonormal basis. Vectors s_1' and s_2' are parallel to the sides of the camera photosensitive matrix, the vector s_3' is perpendicular to the plane of this matrix and directed towards the subject of shooting along optical axes. Hereinafter we will briefly denote this reference frame by video reference frame (VRF).

The reference frames associated with the satellites are shown in Fig. 2.

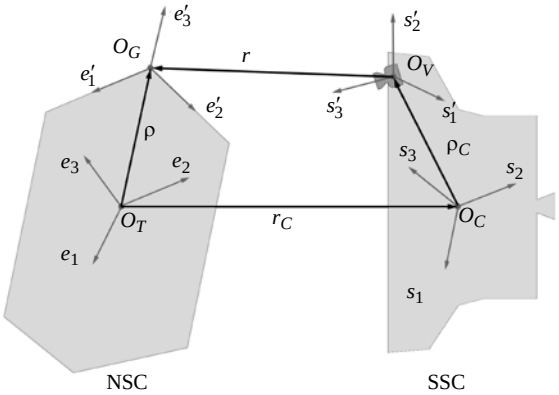

Fig. 2

ISSN 2786-6491

The relative position of two arbitrary coordinate systems can be characterized using a vector pointed from the origin of one coordinate system to the origin of another, and a quaternion characterizing the attitude of the basis of one coordinate system relative to the basis of the other.

1.2. Quaternions. Let us consider some properties of quaternions and operations with them, using [6, 60]. CVS measures quaternion

$$\eta = \eta_0 + \sum_{j=1}^{3} \eta_j s'_j = \eta_0 + \eta_v$$

of attitude of reference frame $O_G E'$ relative to $O_V S'$. The scalar part of the quaternion is determined by the real number η_0, the vector part η_v is characterized by the vector $\eta_v = \sum_{j=1}^{3} \eta_j s'_j$. The numbers η_j, $j = 0:3$, are the coordinates of the quaternion in the basis $O_V s'_1 s'_2 s'_3$. A quaternion η is said to be normalized if its norm

$$\|\eta\| = \eta_0^2 + \eta_1^2 + \eta_2^2 + \eta_3^2 = 1. \tag{1}$$

A normalized quaternion η defines a rotation of three-dimensional Euclidean space R^3 as a whole around an axis defined by a vector $e = \eta_v / \|\eta_v\|$ by an angle φ. In this case $\eta_0 = \cos(\varphi/2)$ and $\eta_v = \sin(\varphi/2)e$. When performing two successive rotations, determined first by the quaternion q, then by quaternion μ, the resulting rotation will be determined by the quaternion

$$\eta = \mu \circ q,$$

where quaternion multiplication $\mu \circ q$ is determined in the following way:

$$\mu \circ q = \mu_0 q_0 - (\mu_v, q_v) + \mu_0 q_v + q_0 \mu_v + \mu_v \times q_v. \tag{2}$$

Here (μ_v, q_v) is a scalar product of vectors μ_v and q_v, $\mu_v \times q_v$ is their vector product. The quaternion coordinates depend on the choice of coordinate system. Therefore, to calculate the quaternion coordinates of η using (2), the quaternion coordinates of q and μ must be expressed in the same coordinate system.

A vector $\eta = (\eta_0, \eta_1, \eta_2, \eta_3)^{\mathrm{T}} \in R^4$ can be formed from the quaternion coordinates of η. We will denote the quaternion and the vector of its coordinates by the same symbol. The same applies to vectors. By virtue of the definition of a normalized quaternion, the vector of its coordinates

$$\eta = (\eta_0, \eta_1, \eta_2, \eta_3)^{\mathrm{T}} = \begin{pmatrix} \cos(\varphi/2) \\ \sin(\varphi/2)\, e \end{pmatrix}. \tag{3}$$

If quaternions $q = (q_0, q_1, q_2, q_3)^{\mathrm{T}}$ and $\mu = (\mu_0, \mu_1, \mu_2, \mu_3)^{\mathrm{T}}$ are represented in the same coordinate system, then using (2), it is easy to obtain the following vector-matrix relations for the quaternion coordinates [6]

$$\eta = \mu \circ q = Q(\mu)\, q = \bar{Q}(q)\, \mu, \tag{4}$$

where 4×4-matrices

$$Q(\mu) = \begin{pmatrix} \mu_0 & -\mu_v^{\mathrm{T}} \\ \mu_v & (\mu_0 I_3 + [\mu_v \times]) \end{pmatrix}, \quad \bar{Q}(q) = \begin{pmatrix} q_0 & -q_v^{\mathrm{T}} \\ q_v & (q_0 I_3 - [q_v \times]) \end{pmatrix}.$$

In this expressions I_3 is unit 3×3-matrix,

$$[q_v\times]=\begin{pmatrix} 0 & -q_3 & q_2 \\ q_3 & 0 & -q_1 \\ -q_2 & q_1 & 0 \end{pmatrix}$$

is matrix of vector cross product, $[q_v\times]\mu_v = q_v\times\mu_v$.

Let x be some vector. Then, with the rotation determined by the quaternion η, the vector x will turn into a vector

$$y = \eta\circ x\circ\overline{\eta},$$

where the vector x should be considered as quaternion with zero scalar part, $\overline{\eta}=\eta_0-\eta_v$ is quaternion conjugate to η, $\eta\circ\overline{\eta}=\overline{\eta}\circ\eta=1$. Conjugate quaternion $\overline{\eta}$, as it follows from its definition and representation (3), determines the rotation around vector e at the angle $-\varphi$, i.e. in the opposite direction. If vector $x=\sum_{j=1}^{3}x_j s'_j$ is given in the basis $s'_j,\ j=1:3,$ by coordinate vector $x=(x_1, x_2, x_3)^{\mathrm{T}}$, then the coordinates of vector $y=\sum_{j=1}^{3}y_j s'_j$ are determined with the use of (4) by the following vector-matrix equality

$$y = R(\eta)\,x \tag{5}$$

where coordinate vector $y=(y_1, y_2, y_3)^{\mathrm{T}}$ and rotation matrix

$$R(\eta)=(\eta_0^2-\eta_v^{\mathrm{T}}\eta_v)I_3+2\eta_0[\eta_v\times]+2\eta_v\eta_v^{\mathrm{T}}. \tag{6}$$

Expression (5) is obtained using the identity

$$Q(\eta)\overline{Q}(\overline{\eta})=\begin{pmatrix} \|\eta\| & \Theta_{1\times3} \\ \Theta_{3\times1} & R(\eta) \end{pmatrix}.$$

Here $\Theta_{m\times n}$ is zero $m\times n$-matrix. It is easy to verify that

$$R(\eta)\,R^{\mathrm{T}}(\eta)=I,\quad R^{\mathrm{T}}(\eta)=R(\overline{\eta}).$$

Quaternion η determines the attitude of $O_G E'$ relative to $O_V S'$ means that the basis vectors $e'_j,\ j=1:3,$ are determined by the following expressions:

$$e'_j=\eta\circ s'_j\circ\overline{\eta},\quad j=1:3,$$

i.e. every basis vector e'_j is obtained by rotation of vector s'_j, and is a linear combination of vectors $s'_j,\ j=1:3$. Obviously, using (5), this can be written as the following formal expression:

$$(e'_1, e'_2, e'_3)=(s'_1, s'_2, s'_3)R(\eta),$$

i.e. j-th column of matrix $R(\eta)$ contains coordinates of the vector e'_j in basis $s'_j,\ j=1:3$. It is easy to obtain from here the inverse relation

$$(s'_1, s'_2, s'_3)=(e'_1, e'_2, e'_3)R(\overline{\eta}).$$

We will often use similar relations in what follows to transform the coordinates of vectors and quaternions. Let us consider quaternions that specify the relative position of the used reference frames.

 ISSN 2786-6491

The attitude of the TRF relative to the IRF is determined by unknown quaternion

$$q = q_0 + \sum_{j=1}^{3} q_j i_j = q_0 + q_v,$$

i.e. the following expression holds for the basis vectors

$$(e_1, e_2, e_3) = (i_1, i_2, i_3)R(q). \tag{7}$$

The attitude of the GRF is determined in the TRF by a constant but unknown quaternion

$$\mu = \mu_0 + \sum_{j=1}^{3} \mu_j e_j = \mu_0 + \mu_v.$$

In this case, the basis

$$(e_1', e_2', e_3') = (e_1, e_2, e_3)R(\mu). \tag{8}$$

The CRF attitude relative to IRF is determined by the known quaternion

$$q_C = q_{C,0} + \sum_{j=1}^{3} q_{C,j} i_j = q_{C,0} + q_{C,v},$$

which is measured with high accuracy, for example, by star trackers. The CRF basis

$$(s_1, s_2, s_3) = (i_1, i_2, i_3)R(q_C). \tag{9}$$

The attitude of the VRF of the video camera relative to the CRF is specified also by the known quaternion

$$\mu_C = \mu_{C,0} + \sum_{j=1}^{3} \mu_{C,j} s_j = \mu_{C,0} + \mu_{C,v}.$$

The VRF basis is determined by the following expression:

$$(s_1', s_2', s_3') = (s_1, s_2, s_3)R(\mu_C). \tag{10}$$

The position of the ORF can be obtained using two rotations of the IRF basis i_j, $j = 1:3$. Let us denote the vector directed from the point O_E (the beginning of the IRF) to the point of the ascending node by a symbol n (see Fig. 1). Obviously, this vector in the IRF is determined by the following expression:

$$n = \cos\Omega i_1 + \sin\Omega i_2 + 0 \cdot i_3.$$

Let us make first rotation around this vector by the orbital inclination angle i, determined by the quaternion

$$q_{1,O} = \left(\cos\frac{i}{2}, \sin\frac{i}{2} n^{\mathrm{T}}\right)^{\mathrm{T}}.$$

As a result of the rotation, the basis i_j, $j = 1:3$, will turn into the basis

$$(i_1', i_2', i_3') = (i_1, i_2, i_3)R(q_{1,O}).$$

According to definition of the ORF we obtain that

$$i_3' = \tau_3 = \sin(i)\sin(\Omega) i_1 - \sin(i)\cos(\Omega) i_2 + \cos(i) i_3.$$

The second rotation is determined by the quaternion

$$q_{2,O} = \begin{pmatrix} \cos\dfrac{[\Omega+\overline{\omega}+\vartheta(t)]}{2} \\ \sin\dfrac{[\Omega+\overline{\omega}+\vartheta(t)]}{2} i_3' \end{pmatrix} = \cos\frac{[\Omega+\overline{\omega}+\vartheta(t)]}{2} + 0\cdot i_1' + 0\cdot i_2' + \sin\frac{[\Omega+\overline{\omega}+\vartheta(t)]}{2} i_3',$$

which is given by coordinates in the basis i_j', $j=1:3$. Here $\vartheta(t)$ is true anomaly angle at the time instant t, measured in the positive direction in the orbital plane from the orbit perigee direction to the direction to the satellite current position. As a result we get

$$(\tau_1, \tau_2, \tau_3) = (i_1', i_2', i_3')R(q_{2,O}) = (i_1, i_2, i_3)R(q_{1,O})R(q_{2,O}) = (i_1, i_2, i_3)R(q_O). \quad (11)$$

where $q_O = q_{2,O} \circ q_{1,O}$. Comparing the expression for q_O and (11), it may seem that the matrices $R(q_{1,O})$ and $R(q_{2,O})$ should be multiplied in the reverse order. Note that in the expression for q_O the quaternion $q_{1,O}$ is specified by coordinates in the basis i_j, $j=1:3$, and the quaternion $q_{2,O}$ is specified in the basis i_j', $j=1:3$. To use vector-matrix representations for operations on quaternions, they must be represented by coordinates in the same coordinate system. By definition, the basis vectors i_j', $j=1:3$, are determined by the following expressions:

$$i_j' = q_{1,O} \circ i_j \circ \overline{q}_{1,O}, \quad j=1:3.$$

Therefore, in the basis i_j, $j=1:3$, quaternion

$$q_{2,O} = q_{2,O(0)} + \sum_{j=1}^{3} q_{2,O(j)} i_j' = q_{1,O} \circ q_{2,O}^* \circ \overline{q}_{1,O},$$

where $q_{2,O}^* = q_{2,O(0)} + \sum_{j=1}^{3} q_{2,O(j)} i_j$. Therefore, the expression for the quaternion q_O in the basis i_j, $j=1:3$, has the following form:

$$q_O = q_{2,O} \circ q_{1,O} = q_{1,O} \circ q_{2,O}^* \circ \overline{q}_{1,O} \circ q_{1,O} = q_{1,O} \circ q_{2,O}^*,$$

which fully corresponds to expression (11). From here for coordinates of the quaternion q_O we obtain

$$q_O = Q(q_{1,O})\, q_{2,O}.$$

Note that the coordinates of the quaternions $q_{2,O}^*$ and $q_{2,O}$ coincide.

Diagram of the relative attitude of the used coordinate systems is shown in Fig. 3.

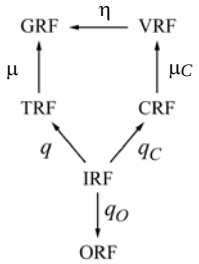

Fig. 3

1.3. Measurement equations. Using the diagram shown in Fig. 3, we can write the following equality

$$\eta \circ \mu_C \circ q_C = \mu \circ q \quad (12)$$

 ISSN 2786-6491

In this expression, the quaternions q_C and μ_C are known, the quaternions q and μ are unknown and must be determined, the quaternion η is measured by the CVS with some limited error. From (12) we obtained

$$\eta = \mu \circ q \circ \overline{q}_C \circ \overline{\mu}_C. \tag{13}$$

To obtain vector-matrix relations corresponding to (13), it is necessary to express the coordinates of all quaternions in VRF, i.e. in the basis $s'_j,\ j = 1:3,$ and apply equality (4). The quaternion μ in the basis $i_j,\ j = 1:3,$ is defined by the following expression:

$$\mu = \mu_0 + \sum_{j=1}^{3} \mu_j e_j = \mu_0 + \sum_{j=1}^{3} \mu_j q \circ i_j \circ \overline{q} = q \circ \left(\mu_0 + \sum_{j=1}^{3} \mu_j i_j\right) \circ \overline{q} = q \circ \mu^* \circ \overline{q}, \tag{14}$$

where $\mu^* = \mu_0 + \sum_{j=1}^{3} \mu_j i_j$. In what follows, we will not put an asterisk over this and similar quaternions, because the coordinates $\mu_j,\ j = 0:3,$ during this and similar basis transformations will be preserved. Substituting (14) into (13), we get

$$\eta = q \circ \mu \circ \overline{q}_C \circ \overline{\mu}_C.$$

The first three factors here are expressed in the basis $i_j,\ j = 1:3.$ Let us transform each of them into a basis $s_j,\ j = 1:3,$ using the identity $i_j = \overline{q}_C \circ s_j \circ q_C,\ j = 1:3.$ As a result we obtain

$$\eta = \overline{q}_C \circ q \circ q_C \circ \overline{q}_C \circ \mu \circ q_C \circ \overline{q}_C \circ \overline{q}_C \circ q_C \circ \overline{\mu}_C = \overline{q}_C \circ q \circ \mu \circ \overline{\mu}_C.$$

In the resulting equality, we proceed to the basis $s'_j,\ j = 1:3,$ in a similar way, using the identity $s_j = \overline{\mu}_C \circ s'_j \circ \mu_C,\ j = 1:3.$ Finally we obtain the following equality:

$$\eta = \overline{\mu}_C \circ \overline{q}_C \circ q \circ \mu. \tag{15}$$

Using Fig. 2, for the vectors characterizing the relative position of the coordinate systems associated with the NSC and the SSC, we can write the following equality:

$$r_C + \rho_C + r = \rho.$$

From here

$$r = \rho - r_C - \rho_C. \tag{16}$$

In this equation $r = O_G - O_V = \sum_{j=1}^{3} r_j s'_j$ is the measured distance vector from the camera to the GRF, $\rho_C = O_V - O_C = \sum_{j=1}^{3} \rho_{C,j} s_j$ is known position of the beginning of the VRF in the CRF, $\rho = O_G - O_T = \sum_{j=1}^{3} \rho_j e_j$ is unknown position of the beginning of the GRF in the TRF, $r_C = O_C - O_T = \sum_{j=1}^{3} r_{C,j} \tau_j = x\tau_1 + y\tau_2 + z\tau_3$ is unknown distance vector from the NSC c.m. to the SSC c.m. in the ORF.

To obtain vector-matrix relations, we express the coordinates of all the vectors in the VRF using equalities (7)–(11). In particular, for the vector ρ_C we obtain

$$\sum_{j=1}^{3} \rho_{C,j} s_j = (s_1, s_2, s_3) \begin{pmatrix} \rho_{C,1} \\ \rho_{C,2} \\ \rho_{C,3} \end{pmatrix} = (s_1, s_2, s_3) \rho_C = (s'_1, s'_2, s'_3) R(\overline{\mu}_C) \rho_C,$$

where $\rho_C = (\rho_{C,1}, \rho_{C,2}, \rho_{C,3})^{\mathrm{T}}$. The elements of a vector $R(\bar{\mu}_C)\rho_C$ are the coordinates of the vector ρ_C in the basis s'_j, $j = 1:3$. Proceeding in a similar way for the remaining vectors of equality (16), it is easy to obtain the following equality for the coordinates:

$$r = R(\bar{\mu}_C)[R(\bar{q}_C)[R(q)\rho - R(q_O)r_C] - \rho_C].$$

We consider the measurements of vector r and quaternion η are made with additive limited errors at discrete times $t_k = t_0 + \Delta \cdot k$, $k = 0, 1, 2, \ldots$, i.e. as a result of the measurement we obtain the following measurement vectors:

$$\breve{r}_k = r(t_k) + \xi_k^r = r_k + \xi_k^r = R(\bar{\mu}_C)[R(\bar{q}_{C,k})[R(q_k)\rho - R(q_{O,k})r_{C,k}] - \rho_C] + \xi_k^r, \quad (17)$$

$$\breve{\eta}_k = \eta(t_k) + \xi_k^\eta = \eta_k + \xi_k^\eta = \bar{\mu}_C \circ \bar{q}_{C,k} \circ q_k \circ \mu_k + \xi_k^\eta = Q(\bar{\mu}_C)Q(\bar{q}_{C,k})\bar{Q}(\mu_k)q_k + \xi_k^\eta. \quad (18)$$

For measurement errors, only their maximum values are known, i.e. such numbers $c_r > 0$ and $c_\eta > 0$ for which the following inequalities hold:

$$\| \xi_k^r \|_\infty \le c_r, \ \| \xi_k^\eta \|_\infty \le c_\eta.$$

From here, (17) and (18) it follows that the unknown parameters of the NSC motion satisfy the following inequalities:

$$\| \breve{r}_k - R(\bar{\mu}_C)R(\bar{q}_{C,k})R(q_k)\rho + R(\bar{\mu}_C)R(\bar{q}_{C,k})R(q_{O,k})r_{C,k} + R(\bar{\mu}_C)\rho_C \|_\infty \le c_r,$$

$$\| \breve{\eta}_k - Q(\bar{\mu}_C)Q(\bar{q}_{C,k})\bar{Q}(\mu_k)q_k \|_\infty \le c_\eta. \quad (19)$$

1.4. Dynamical equations. The change in time of the quaternion coordinates $q = (q_1, q_2, q_3, q_4)^{\mathrm{T}}$ is described by the following equation [6, 60]:

$$\dot{q} = \frac{1}{2} q \circ \omega = \frac{1}{2} Q_v(q)\omega, \quad (20)$$

where the NSC angular velocity $\omega = (\omega_1, \omega_2, \omega_3)^{\mathrm{T}}$ is given in the TRF and 4×3-matrix

$$Q_v(q) = \begin{pmatrix} -q_v^{\mathrm{T}} \\ q_0 I_3 + [q_v \times] \end{pmatrix}.$$

Vector ω satisfies the following equation [60, 6]:

$$J\frac{d\omega}{dt} + [\omega \times] J\omega = M. \quad (21)$$

The inertia tensor matrix J in this equation has a diagonal form

$$J = \mathrm{diag}(J_1, J_2, J_3).$$

The main inertia moments J_i, $i = 1:3$, are considered to be unknown. The moment M in equation (21) may include gravitational moment, aerodynamic and other moments caused by the action of the environment on the NSC [32]. We will assume that the influence of these moments on the NSC angular position during the observation time can be neglected, i.e. in equation (21) we assume

$$M = 0.$$

 ISSN 2786-6491

It is easy to verify that in the absence of a moment of external forces, the solutions of equation (21) depend only on the ratios of the inertia moments. Let us introduce the following notation [35]:

$$l_1 = \frac{J_2 - J_3}{J_1}, l_2 = \frac{J_3 - J_1}{J_2}, l_3 = \frac{J_1 - J_2}{J_3}.$$

Then equations (21) can be written in the following component form:

$$\begin{cases} \dot{\omega}_1 = l_1 \omega_2 \omega_3; \\ \dot{\omega}_2 = l_2 \omega_1 \omega_3; \\ \dot{\omega}_3 = l_3 \omega_1 \omega_2. \end{cases} \tag{22}$$

We assume that over the considered period of time the inertia moments are constant. Therefore, for the vector $l = (l_1, l_2, l_3)^{\mathrm{T}}$ it holds

$$\dot{l} = 0. \tag{23}$$

The coordinates of the vector ρ and quaternion μ in the corresponding coordinate systems are also constant. Therefore we assume

$$\dot{\rho} = (\dot{\rho}_1, \dot{\rho}_2, \dot{\rho}_3)^{\mathrm{T}} = 0; \;\; \dot{\mu} = (\dot{\mu}_1, \dot{\mu}_2, \dot{\mu}_3, \dot{\mu}_4)^{\mathrm{T}} = 0. \tag{24}$$

Let the SSC be located at a short distance from the NSC, i.e. for coordinates of the vector

$$r_C = x\tau_1 + y\tau_2 + z\tau_3$$

the following condition holds:

$$x^2 + y^2 + z^2 << r_T^2,$$

where $r_T = r_T(t)$ is the distance from the Earth c.m. to the NSC c.m. Then the change in coordinates of vector r_C can be described by the following linear equation [59, p. 679]:

$$\begin{cases} \ddot{x} - x\omega_O^2 \left(1 + 2\frac{r_T}{p}\right) - 2\omega_O \left(\dot{y} - y\frac{\dot{r}_T}{r_T}\right) = a_x; \\ \ddot{y} + 2\omega_O \left(\dot{x} - x\frac{\dot{r}_T}{r_T}\right) - y\omega_O^2 \left(1 - \frac{r_T}{p}\right) = a_y; \\ \ddot{z} + \frac{r_T}{p}\omega_O^2 z = a_z. \end{cases}$$

Here $\omega_O = \omega_O(t) = \dot{\vartheta}(t)$ is the absolute angular velocity of rotation of the ORF, $p = 2r_p r_a / (r_p + r_a)$ is the orbit focal parameter [61], r_a is the orbit apogee, r_p is the orbit perigee, a_x, a_y and a_z are the acceleration projections on the axes of the ORF, created by external forces acting on the SSC, which are assumed to be known. Let's write these equations in the following form:

$$\begin{cases} \dot{r}_C = v_C, \\ \dot{v}_C = A_r(\omega_O, r_T, p) r_C + A_v(\omega_O) v_C + a. \end{cases} \tag{25}$$

Here $r_C = (x, y, z)^{\mathrm{T}}$ is the vector of the SSC relative position, $v_C = (\dot{x}, \dot{y}, \dot{z})^{\mathrm{T}}$ is the vector of relative velocities, $a = (a_x, a_y, a_z)^{\mathrm{T}}$ is acceleration vector, matrices

$$A_r(\omega_O, r_T, p) = \begin{pmatrix} \omega_O^2(1+2r_T p^{-1}) & -2\omega_O \dot{r}_T r_T^{-1} & 0 \\ 2\omega_O \dot{r}_T r_T^{-1} & \omega_O^2(1-r_T p^{-1}) & 0 \\ 0 & 0 & -\omega_O^2 r_T p^{-1} \end{pmatrix},$$

$$A_v(\omega_O) = \begin{pmatrix} 0 & 2\omega_O & 0 \\ -2\omega_O & 0 & 0 \\ 0 & 0 & 0 \end{pmatrix}.$$

To integrate equation (25), it is necessary to know $\omega_O = \dot{\vartheta}(t)$, $r_T(t)$ and $\dot{r}_T(t)$. We will assume that the value of the true anomaly $\vartheta_0 = \vartheta(t_0)$ for the initial time t_0, is known. Then $\dot{\vartheta}(t)$ is determined by integrating the following equation [61]:

$$\dot{\vartheta}(t) = C r_T^{-2} = C(1+e\cos\vartheta(t))^2 p^{-2}.$$

Values of $r_T(t)$ and $\dot{r}_T(t)$ are determined by the formulas

$$r_T(t) = p(1+e\cos\vartheta(t))^{-1}, \quad \dot{r}_T(t) = Cp^{-1}e\sin\vartheta(t),$$

and considered to be known. In these equations $e = (r_a - r_p)/(r_a + r_p)$ is the orbit eccentricity, $C = \sqrt{\mu_E p}$, μ_E is the Earth gravitational constant [61].

1.5. Problem statement. Differential equations (20)–(25) can be considered as equations of a nonlinear dynamic system in continuous time with the following state vector:

$$x = (q^{\mathrm{T}}, \omega^{\mathrm{T}}, r_C^{\mathrm{T}}, v_C^{\mathrm{T}}, l^{\mathrm{T}}, \rho^{\mathrm{T}}, \mu^{\mathrm{T}})^{\mathrm{T}}. \tag{26}$$

The initial conditions for these equations are unknown. At discrete moments of time, some components of this vector $x_k = x(t_k) = (q_k^{\mathrm{T}}, \omega_k^{\mathrm{T}}, r_{C,k}^{\mathrm{T}}, v_{C,k}^{\mathrm{T}}, l_k^{\mathrm{T}}, \rho_k^{\mathrm{T}}, \mu_k^{\mathrm{T}})^{\mathrm{T}}$ must satisfy inequalities (19) associated with measurements. In addition, normalization conditions (1) must be satisfied for the components q and μ.

Let $\hat{x}_{k-1}$ be some estimate of the state vector x_{k-1} obtained at the moment of discrete time $(k-1)$. Using this value as the initial value for differential equations (20)–(25), we can calculate the estimate $\hat{x}_{k|k-1}$ for the moment k. If this estimate satisfies inequalities (19), then, obviously, there is no need to refine it and we can put $\hat{x}_k = \hat{x}_{k|k-1}$. If the estimate $\hat{x}_{k|k-1}$ does not satisfy at least one of the inequalities (19), then its clarification is required.

The problem is to find a method for refining estimates $\hat{x}_{k|k-1}$ in which inequalities (19) will be satisfied for estimates $\hat{x}_{k|k-1}$ starting from some finite moment K and, therefore, from this moment the refinement is not required. Ideally, this method should provide existence of the limit

$$\lim_{k\to\infty} \| \hat{x}_k - x_k \| = 0.$$

ISSN 2786-6491

Its existence is associated with the absence of uncontrollable disturbances in the system under consideration, and with realization of certain properties of measurement noise, which is difficult to verify and ensure in practice.

2. Method for solving the estimation problem

In this work we use a minimum of information about uncertain quantities, which is almost always available in practice. Thus, for measurement noise, only its maximum possible value is assumed to be known. The state vector is unknown, but it must satisfy inequalities associated with measurement equations and noise magnitude constraints. In fact, the unknown state vector belongs to the set defined by these inequalities. Therefore, the estimation procedure comes down to constructing so-called information sets that are guaranteed to contain true estimated values.

In this work, we use one of the modifications [54, 55] of the guaranteed estimation algorithm using ellipsoids. The main advantages of this method are the high speed of convergence, applicability to nonlinear systems, and resistance to possible violations of a priori hypotheses.

2.1. Guaranteed approach to state vector estimation of dynamic systems. Equations (20)–(25), using definition (26) of the state vector, can be written in the form

$$\dot{x} = f(x(t), u(t), \zeta(t)), t \geq t_0, \tag{27}$$

where $x(t) \in R^n$ is the state vector at a moment of continuous time t (R^n is n-dimensional real Euclidean space), $u(t) \in R^m$ is the vector of measured input variables, $\zeta(t) \in R^d$ is the vector of uncontrolled disturbances. In this case, this may be the moment vector M in equation (21) acting on the NSC. We assume that the functions $f(\cdot)$, $u(\cdot)$ and $\zeta(\cdot)$ in (27), satisfy the standard conditions of existence and uniqueness of solution of ordinary differential equations [62]. The vector

$$\zeta(t) \in Z \subset R^d \quad \forall t, \tag{28}$$

where Z is some bounded closed set.

The measurement inequalities (19) can be written in the following form:

$$\left| y_{j,k} - g_j(x_k) \right| \leq c_j, \quad j = 1:N, \tag{29}$$

where $y_{j,k}$, c_j and $g_j(x)$ are the measurement values of the j-th output variable, the value of the maximum measurement noise of this variable and the continuously differentiable measurement function, respectively, $j = 1:N$, $N = 7$. In addition, for quaternions included in the state vector, the normalization condition (1) must be satisfied.

Let us describe the procedure for updating information on the state vector in accordance with the guaranteed (set-theoretic) approach to estimation using ellipsoids. Let us assume that at the moment t_k it is known that the state vector

$$x_k = x(t_k) \in E_k, \tag{30}$$

where the ellipsoid

$$E_k = E(\hat{x}_k, H_k) = \{x : (x - \hat{x}_k)^{\mathrm{T}} H_k^{-1} (x - \hat{x}_k) \leq 1\},$$

characterized by a center vector $\hat{x}_k$ and a positive definite symmetric matrix $H_k = H_k^T > 0$. The ellipsoid E_k in (30) is usually called the set or ellipsoidal estimate of the vector x_k. The center of the ellipsoid, the vector $\hat{x}_k$ is taken as a point estimate.

Considering equation (27) on a time interval $[t_k, t_{k+1}]$ for all possible initial conditions satisfying (30), and for all possible implementations of disturbances $\zeta(\cdot)$ satisfying condition (28) on this interval, we can obtain the set

$$X_{k+1|k} = \{x = x(t_{k+1}, x_k, u(\cdot), \xi(\cdot)), \forall x_k \in E_k \ \forall \zeta(\tau) \in Z \ \forall \tau \in [t_k, t_{k+1}]\}$$

of possible values of the vector $x_{k+1} = x(t_{k+1})$ at a discrete moment $k+1$. The set $X_{k+1|k}$ is not in general an ellipsoid. The construction of this set can be carried out, for example, by integrating the system equation (27) over the interval $[t_k, t_{k+1}]$ under various initial conditions satisfying (30) and for all possible implementations of disturbances $\zeta(\tau) \in Z \ \forall \tau \in [t_k, t_{k+1}]$. Obviously, this is a very labor-intensive process that requires a large number of calculations.

On the other hand, the state vector x_{k+1} satisfies inequalities (29) at the time moment t_{k+1}, which can be written in the form

$$x_{k+1} \in \bar{X}_{k+1} = \bigcap_{j=1}^{N} \bar{X}_{j,k+1}.$$

where the set

$$\bar{X}_{j,k+1} = \{x : \left| y_{j,k+1} - g_j(x) \right| \le c_j\}. \tag{31}$$

The set $\bar{X}_{k+1}$ contains state vectors that are compatible with measurements under given a priori bounds on the measurement noise. As a result, we can conclude that

$$x_{k+1} \in X_{k+1} = \bar{X}_{k+1} \bigcap X_{k+1|k}.$$

Despite the obvious simplicity and logical rigor of the presented approach for updating the set of possible values of the state vector, its practical implementation in general encounters insurmountable computational difficulties associated with the construction and description of the sets $X_{k+1|k}$, $\bar{X}_{k+1}$, X_{k+1}, as well as the implementation of set-theoretic operations, in the considered case, the set intersection operation.

One of the approaches aimed at reducing the computational complexity of solving estimation problems is to use the ellipsoid method [42–53]. In accordance with this method, approximations are constructed for the sets $X_{k+1|k}$ and X_{k+1} in the form of containing them ellipsoids $E_{k+1|k} = E(\hat{x}_{k+1|k}, H_{k+1|k})$ and $E_{k+1} = E(\hat{x}_{k+1}, H_{k+1})$, and the solution to the estimation problem is reduced to constructing a sequence of ellipsoidal estimates $\{E_k\}_{k=0}^{\infty}$, $x_k \in E_k$, for the vector x_k in accordance with the following recurrent procedure:

$$x_{k+1} \in E_{k+1} = [\bar{X}_{k+1} \bigcap [X_{k+1|k}]_E]_E = [\bar{X}_{k+1} \bigcap E_{k+1|k}]_E. \tag{32}$$

Here $[X]_E$ denotes the operation of covering a bounded set $X \subset R^n$ by minimal in a certain sense ellipsoid E, i.e. $X \subset E$. The criterion for choosing such an ellipsoid is usually its volume, diameter, or other function characterizing the ellipsoid size. The described method for constructing ellipsoidal estimates is called ellipsoidal estimation. The advantage of scheme (32) compared to the initial scheme is that set-theoretic operations are performed on sets of a fixed structure, but the disadvantage is that the covering ellipsoids have a larger size than the covered sets, i.e. ellipsoids contain extra areas.

For linear systems, many standard operations $[X]_E$ have been developed, optimal and suboptimal in some sense [42, 43]. In the case of nonlinear systems, the operation $[X]_E$ can, in general, be implemented only numerically and requires a large amount of calculations. In particular, this applies to the analogue of the unscented Kalman filter [49, 50], in which the image of the ellipsoid under nonlinear transformation is obtained as a minimal in some sense ellipsoid, containing images of specially selected points in the initial ellipsoid E_k. There are methods for constructing an ellipsoid $E_{k+1|k}$ based on the use of the Taylor series expansion of a nonlinear function $f(\cdot)$ up to second order [47, 48]. The ellipsoidal estimates obtained in this case are very rough, i.e. their sizes can significantly exceed the sizes of the set $X_{k+1|k}$ that can negatively affect the convergence of an estimation method based on such approximations. The work [51] proposes a method for constructing a sequence of volume-optimal ellipsoidal estimates for the case of nonlinear polynomial systems. However, even with dimension two, the computational costs of implementing this method are very high.

In [54, 55], a modification of the ellipsoidal estimation method was considered, which makes it possible to reduce the amount of calculations when constructing a sequence of ellipsoidal estimates, and at the same time significantly increase the speed of convergence, and also give the estimation algorithm the property of robustness with respect to violations of a priori assumptions about the properties of uncertain quantities of the estimation problem. A similar approach was previously proposed and studied in [52, 53]. In accordance with [55], the ellipsoid $E_{k+1|k}$ is constructed, as in the extended Kalman filter, with the use of the linear part of the expansion of the function in (27) in the vicinity of the point $\hat{x}_k$. The center vector $\hat{x}_{k+1|k}$ of the ellipsoid $E_{k+1|k}$ is found by numerically integrating the following equation:

$$d\tilde{x}/dt = f(\tilde{x}(t), u(t), \hat{\zeta}(t)),\ \tilde{x}(t_k) = \hat{x}_k,\ t \in [t_k, t_{k+1}],$$

taking $\hat{x}_{k+1|k} = \tilde{x}(t_{k+1})$. Here $\hat{\zeta}(t)$ is some estimate of unknown vector $\zeta(t)$, chosen from some considerations. Usually people takes $\hat{\zeta}(t) = 0$.

The condition (30) can be written in the form

$$\Delta x_k = x_k - \hat{x}_k \in \Delta E_k,$$

where ellipsoid $\Delta E_k = E(0, H_k) = \{\Delta x : \Delta x^{\mathrm{T}} H_k^{-1} \Delta x \le 1\}$. Let us consider construction of approximate ellipsoidal estimate for $\Delta x_{k+1|k} = x_{k+1} - \hat{x}_{k+1|k}$. At the interval $[t_k, t_{k+1}]$ for the value

$$\Delta x(t) = x(t) - \tilde{x}(t),$$

we can obtain with the use of the Taylor series expansion of function $f(x(t), u(t), \zeta(t))$ at vicinity of $\tilde{x}(t)$ and $\hat{\zeta}(t)$ the following equation:

$$\frac{d\Delta x}{dt} = \partial_x f(\tilde{x}(t), u(t), \hat{\zeta}(t))\Delta x + \partial_\zeta f(\tilde{x}(t), u(t), \hat{\zeta}(t))\Delta\zeta(t) +$$

$$+ o_x(\|\Delta x\|) + o_\zeta(\|\Delta\zeta\|),\ t \in [t_k, t_{k+1}]. \qquad (33)$$

Here the functions $o_x(\|\Delta x\|)$ and $o_\zeta(\|\Delta\zeta\|)$ denote the terms of the expansion of the second order of smallness. This equation, using various estimates, in principle allows to calculate the matrix $H_{k+1|k}$ of the ellipsoid $\Delta E_{k+1|k} = E(0, H_{k+1|k}),\ \Delta x_{k+1|k} \in \Delta E_{k+1|k}$. However, the computational costs can be quite large. Therefore, it is proposed [55] to use instead of (33) the following approximate, but simple stationary linear equation:

$$\frac{d\Delta x}{dt} = A_k \Delta x,\ \ t \in [t_k, t_{k+1}], \tag{34}$$

where $n \times n$-matrix

$$A_k = \partial_x f(\hat{x}_{k+1/2}, u_{k+1/2}, \hat{\zeta}_{k+1/2}).$$

Here

$$\hat{x}_{k+1/2} = 0,5 \cdot (\hat{x}_{k+1|k} + \hat{x}_k),\ \ u_{k+1/2} = \frac{1}{\Delta}\int_{t_k}^{t_{k+1}} u(\tau)\, d\tau,\ \ \hat{\zeta}_{k+1/2} = \frac{1}{\Delta}\int_{t_k}^{t_{k+1}} \hat{\zeta}(\tau)\, d\tau.$$

Since $\Delta x_k \in E(0, H_k),$ then by virtue of equation (34) we can obtain [52] that

$$\Delta x_{k+1|k} = \Delta x(t_{k+1}) \in E(0, H_{k+1|k}),$$

where

$$H_{k+1|k} = \mathrm{A}_k H_k \mathrm{A}_k^{\mathrm{T}}, \tag{35}$$

and $n \times n$-matrix $\mathrm{A}_k = \exp(A_k \cdot \Delta).$ Finally we get

$$E_{k+1|k} = E(x_{k+1|k}, H_{k+1|k}) = \{x : (x - \hat{x}_{k+1|k})^{\mathrm{T}} H_{k+1|k}^{-1} (x - \hat{x}_{k+1|k}) \le 1\}.$$

Due to the use of approximate equation (34) $E_{k+1|k} \ne X_{k+1|k}$, i.e. some ends of the trajectories of system (27), coming out of the set E_k, will not belong to this $E_{k+1|k}$.

Instead of a set $\overline{X}_{k+1}$ in (32), its estimate is also considered

$$\hat{X}_{k+1} = \bigcap_{j=1}^{N} \Pi_{j,k+1},$$

where the sets

$$\Pi_{j,k+1} = \{x : | y_{j,k+1} - g_j(\hat{x}_{k+1|k}) - \nabla g_j^{\mathrm{T}}(\hat{x}_{k+1|k})(x - \hat{x}_{k+1|k})| \le c_j\} \tag{36}$$

are obtained by replacing the function $g_j(x)$ in (31) with its linear approximation in the vicinity of the point $\hat{x}_{k+1|k}$. From (36) it follows that if $\hat{x}_{k+1|k} \in \overline{X}_{j,k+1}$, then $\hat{x}_{k+1|k} \in \Pi_{j,k+1}$, and vice versa. However, the set $\hat{X}_{k+1} \ne \overline{X}_{k+1}$. Due to this and the fact that $E_{k+1|k} \ne X_{k+1|k}$, it may turn out that $E_{k+1|k} \cap \hat{X}_{k+1} = \varnothing,$ and it is impossible then to implement an analogue of scheme (32) for constructing an ellipsoid E_{k+1} in the form $E_{k+1} = [E_{k+1|k} \cap \hat{X}_{k+1}]_E$. Therefore, in this case $E_{k+1|k} \cap \hat{X}_{k+1} = \varnothing,$ it is proposed to take instead of an ellipsoid $E_{k+1|k}$, the ellipsoid of increased size

$$\tilde{E}_{k+1|k} = \{x : (x - \hat{x}_{k+1|k})^{\mathrm{T}} \tilde{H}_{k+1|k}^{-1} (x - \hat{x}_{k+1|k}) \le 1\}, \tag{37}$$

where matrix

$$\tilde{H}_{k+1|k} = \alpha^2 H_{k+1|k}.$$

The number $\alpha > 1$ is chosen in such a way that the set $\tilde{E}_{k+1|k} \bigcap \hat{X}_{k+1} \neq \varnothing$ is the body. Formulas for selection of α and necessary explanations are given in [54, 55]. The ellipsoid E_{k+1} covering the intersection $\tilde{E}_{k+1|k} \bigcap \hat{X}_{k+1}$ can be obtained using standard iterative procedures [42, 52, 53]. In this work, the construction of the ellipsoid E_{k+1} is carried out iteratively [54] in accordance with the scheme

$$E_{s+1} = [E_s \bigcap \Pi_{s \bmod N+1,k+1}]_E \quad s = 0, 1, 2, \ldots$$

The ellipsoid $E_{k+1|k}$ is taken as the initial ellipsoid $E_{s=0}$, i.e. $E_{s=0} = E_{k+1|k}$. In this case, the operation $[\cdot]_E$ of constructing an ellipsoid of minimal volume containing the intersection $E_s \bigcap \Pi_{s \bmod N+1,k}$ of the ellipsoid E_s and a multidimensional layer $\Pi_{s \bmod N+1,k}$, is used. If it turns out that $E_s \bigcap \Pi_{s \bmod N+1,k} = \varnothing$, then the ellipsoid matrix H_s is multiplied by a factor α_s^2 that ensures deepening the ellipsoid $\tilde{E}_s$ into a multidimensional layer $\Pi_{s \bmod N+1,k}$ to a depth of δ. The process of constructing ellipsoids E_s will stop [54] at some finite $s = S$. In this case, the inclusion $x_S \in \in \bigcap_{j=1}^{N} \Pi_{j,k+1}$ is true for the center x_S of the resulting ellipsoid $E_S = E(x_S, H_S)$. Finally we assume $E_{k+1} = E_S$.

Note that in notations (36) and (37) the quantity $\Delta x = x - \hat{x}_{k+1|k}$ appears as a variable. Therefore, the above algorithm can be considered as search of an increment $\Delta x_{k+1} = \hat{x}_{k+1} - \hat{x}_{k+1|k}$.

2.2. Linearization of the equations. We use the multiplicative form of quaternion increment [56, 57], so quaternion q is written as

$$q = \hat{q} \circ \Delta q, \tag{38}$$

where $\hat{q}$ is an estimate and Δq is the estimate error. This representation allows us to avoid the need for forced normalization of product if both its factors $\hat{q}$ and Δq are normalized. Moreover, if we assume that the quaternion Δq is small, i.e. determines a rotation at a small angle φ $(\varphi \approx 0)$ around some unknown axis e, $\|e\| = 1$, then, in accordance with the quaternion representation in the form (3), the following estimates will be valid

$$\Delta q_0 \approx 1, \quad \|\Delta q_v\| \approx 0. \tag{39}$$

Knowing the vector part Δq_v, we can determine from the normalization condition the scalar part in accordance with the expression

$$\Delta q_0 = \sqrt{1 - \|\Delta q_v\|^2}, \tag{40}$$

i.e. a quaternion Δq is completely characterized by its vector part.

In expression (15) for the quaternion η, we will use representation (38) for the quaternion q and the representation

$$\mu = \Delta\mu \circ \hat{\mu}$$

for the quaternion μ [34, 35]. The sense of choosing such a representation will be clear from what follows. The use of the vector part of quaternions Δq and $\Delta\mu$ allows to reduce the dimension of the state vector at estimation, and to normalize them using formula (40).

When using the vector part Δq_v and $\Delta\mu_v$ to specify quaternion increments, the state vector increment

$$\Delta x = (\Delta q^{\mathrm{T}},\ \Delta\omega^{\mathrm{T}},\ \Delta r_C^{\mathrm{T}},\ \Delta v_C^{\mathrm{T}},\ \Delta l^{\mathrm{T}},\ \Delta\rho^{\mathrm{T}},\ \Delta\mu^{\mathrm{T}})^{\mathrm{T}} \in R^{23}$$

is uniquely characterized by the following vector of lower dimension:

$$\delta x = (\Delta q_v^{\mathrm{T}},\ \Delta\omega^{\mathrm{T}},\ \Delta r_C^{\mathrm{T}},\ \Delta v_C^{\mathrm{T}},\ \Delta l^{\mathrm{T}},\ \Delta\rho^{\mathrm{T}},\ \Delta\mu_v^{\mathrm{T}})^{\mathrm{T}} \in R^{21}.$$

Therefore, knowledge of δx_{k+1} is sufficient to calculate in accordance with the measurement results the increment Δx_{k+1} for updating the estimate $\hat{x}_{k+1|k}$ at the moment $(k+1)$.

We obtain a linear differential equations that approximately describe the evolution of the vector δx. For equations (22), assuming $\omega(t) = \tilde{\omega}(t) + \Delta\omega(t)$, $l(t) = \tilde{l}(t) + \Delta l(t)$, we obtain

$$\begin{cases} \Delta\dot{\omega}_1 = \tilde{l}_1(\Delta\omega_2\tilde{\omega}_3 + \tilde{\omega}_2\Delta\omega_3) + \Delta l_1\tilde{\omega}_2\tilde{\omega}_3; \\ \Delta\dot{\omega}_2 = \tilde{l}_2(\Delta\omega_1\tilde{\omega}_3 + \tilde{\omega}_1\Delta\omega_3) + \Delta l_2\tilde{\omega}_1\tilde{\omega}_3; \\ \Delta\dot{\omega}_3 = \tilde{l}_3(\Delta\omega_1\tilde{\omega}_2 + \tilde{\omega}_1\Delta\omega_2) + \Delta l_3\tilde{\omega}_1\tilde{\omega}_2; \end{cases}$$

which we write in matrix notations

$$\Delta\dot{\omega} = A_{\omega}(\tilde{\omega}, \tilde{l})\Delta\omega + A_l(\tilde{\omega})\Delta l. \tag{41}$$

Here the matrices

$$A_{\omega}(\omega, l) = \begin{pmatrix} 0 & l_1\omega_3 & l_1\omega_2 \\ l_2\omega_3 & 0 & l_2\omega_1 \\ l_3\omega_2 & l_3\omega_1 & 0 \end{pmatrix},\ A_l(\omega) = \begin{pmatrix} \omega_2\omega_3 & 0 & 0 \\ 0 & \omega_1\omega_3 & 0 \\ 0 & 0 & \omega_1\omega_2 \end{pmatrix}.$$

Using the equation (20), we obtain differential equation for Δq_v. Considering $\tilde{q}$ as estimate of q from (38) we get $\Delta q = \bar{\tilde{q}} \circ q$. Differentiating this expression, we have

$$\Delta\dot{q} = \dot{\bar{\tilde{q}}} \circ q + \bar{\tilde{q}} \circ \dot{q}. \tag{42}$$

Let us differentiate the identity $\tilde{q} \circ \bar{\tilde{q}} = 1$, then we get $\dot{\tilde{q}} \circ \bar{\tilde{q}} + \tilde{q} \circ \dot{\bar{\tilde{q}}} = 0$. From here

$$\dot{\bar{\tilde{q}}} = -\bar{\tilde{q}} \circ \dot{\tilde{q}} \circ \bar{\tilde{q}}. \tag{43}$$

On definition

$$\dot{\tilde{q}} = 0{,}5\tilde{q} \circ \tilde{\omega}.$$

Substituting this expression into (43), and then the resulting equality into (42), taking into account (2), we obtain

$$\Delta\dot{q} = \bar{\tilde{q}} \circ \dot{q} - \bar{\tilde{q}} \circ \dot{\tilde{q}} \circ \bar{\tilde{q}} \circ q = 0{,}5\bar{\tilde{q}} \circ \tilde{q} \circ \Delta q \circ (\tilde{\omega} + \Delta\omega) - 0{,}5\bar{\tilde{q}} \circ \tilde{q} \circ \tilde{\omega} \circ \bar{\tilde{q}} \circ \tilde{q} \circ \Delta q =$$

$$= 0{,}5(\Delta q \circ \tilde{\omega} - \tilde{\omega} \circ \Delta q) + 0{,}5\Delta q \circ \Delta\omega = -[\tilde{\omega}\times]\Delta q_v + 0{,}5\bar{Q}(\Delta\omega)\Delta q. \tag{44}$$

 ISSN 2786-6491

Let's evaluate the right side of this equation. Neglecting terms of smallness order higher than the first, using the expression for the matrix $\bar{Q}(q)$ and estimate (39), we get

$$\bar{Q}(\Delta\omega)\Delta q = \begin{pmatrix} 0 & -\Delta\omega^{\mathrm{T}} \\ \Delta\omega & -[\Delta\omega\times] \end{pmatrix} \begin{pmatrix} \Delta q_0 \\ \Delta q_v \end{pmatrix} \approx \begin{pmatrix} 0 \\ \Delta\omega \end{pmatrix}.$$

Taking into account the last equality, from (44) we obtain

$$\Delta\dot{q}_v \approx -[\tilde{\omega}\times]\Delta q_v + 0,5\Delta\omega,\ \Delta\dot{q}_0 \approx 0. \tag{45}$$

Equations (25) are linear. Therefore, for them we can immediately write

$$\begin{cases} \Delta\dot{r}_C = \Delta v_C, \\ \Delta\dot{v}_C = A_r(\omega_O, r_T, p)\Delta r_C + A_v(\omega_O)\Delta v_C. \end{cases}$$

For constant parameters l, ρ and μ, the following equations are obviously valid:

$$\Delta\dot{l} = 0,\ \Delta\dot{\rho} = 0,\ \Delta\dot{\mu}_v = 0. \tag{46}$$

Combining equations (41), (45) and (46), we obtain an equation that describes the change in time of the vector δx in the linear approximation

$$\delta\dot{x} = \begin{pmatrix} A(\tilde{x}) & \Theta_{15\times 6} \\ \Theta_{6\times 15} & \Theta_{6\times 6} \end{pmatrix} \delta x, \tag{47}$$

where 15×15-matrix

$$A(x) = \begin{pmatrix} -[\omega\times] & 0,5I_3 & \Theta_{3\times 3} & \Theta_{3\times 3} & \Theta_{3\times 3} \\ \Theta_{3\times 3} & A_\omega(\omega, l) & \Theta_{3\times 3} & \Theta_{3\times 3} & A_l(\omega) \\ \Theta_{3\times 3} & \Theta_{3\times 3} & \Theta_{3\times 3} & I_3 & \Theta_{3\times 3} \\ \Theta_{3\times 3} & \Theta_{3\times 3} & A_r(\omega_O, r_T, p) & A_v(\omega_O) & \Theta_{3\times 3} \\ \Theta_{3\times 3} & \Theta_{3\times 3} & \Theta_{3\times 3} & \Theta_{3\times 3} & \Theta_{3\times 3} \end{pmatrix}.$$

Let us assume that at the moment t_k for the vector δx the following inclusion holds:

$$\delta x(t_k) = \delta x_k \in \delta E_k = E(0, H_k).$$

In accordance with the approach outlined in subsection 2.1, for the matrix A_{k+1} used in calculating the matrix $H_{k+1|k}$ of ellipsoid $\delta E_{k+1|k} = E(0, H_{k+1|k})$, by virtue of (47) we take the following expression:

$$\mathrm{A}_{k+1} = \begin{pmatrix} e^{A_{k+1/2}\Delta} & \Theta_{15\times 6} \\ \Theta_{6\times 15} & I_6 \end{pmatrix}, \tag{48}$$

Here $A_{k+1/2}$ is the value of the matrix $A(x)$ at the following values of its arguments $\hat{\omega}_{k+1/2} = 0,5(\hat{\omega}_{k+1|k} + \hat{\omega}_k)$, $\hat{l}_k$, $r_{T,k+1/2} = 0,5(r_{T,k+1} + r_{T,k})$, and $\omega_{O,k+1/2} = 0,5(\omega_{O,k+1} + \omega_{O,k})$. The ellipsoid δE_k $(\delta E_k \subset R^{21})$ contains the possible values of the vector δx_k, and the ellipsoid $\delta E_{k+1|k}$ contains the possible values of the vector $\delta x_{k+1|k}$.

Let us linearize the functions $g_j(x)$ appearing in measurement equations (17) and (18) in the point $\hat{x}_{k+1|k}$ with respect to δx. To do this, substitute an expression for the state vector expressed in terms of estimates and their increments, into these function expressions. The terms which are linear with respect to δx, will contain the desired gradients of functions $g_j(x)$.

For equation (17), considered for the moment $(k+1)$, we have

$$\breve{r}_{k+1} = R(\bar{\mu}_C)R(\bar{q}_{C,k+1})R(\hat{q}_{k+1|k} \circ \Delta q)(\hat{\rho}_{k+1|k} + \Delta\rho) - R(\bar{\mu}_C)R(\bar{q}_{C,k+1})R(q_{O,k+1}) \times$$

$$\times(\hat{r}_{C,k+1|k} + \Delta r_C) - R(\bar{\mu}_C)\rho_C + \xi^r_{k+1} = R(\bar{\mu}_C)R(\bar{q}_{C,k+1})R(\hat{q}_{k+1|k})R(\Delta q)(\hat{\rho}_{k+1|k} + \Delta\rho) -$$

$$-R(\bar{\mu}_C)R(\bar{q}_{C,k+1})R(q_{O,k+1})(\hat{r}_{C,k+1|k} + \Delta r_C) - R(\bar{\mu}_C)\rho_C + \xi^r_{k+1} \approx$$

$$\approx R(\bar{\mu}_C)R(\bar{q}_{C,k+1})R(\hat{q}_{k+1|k})(I_3 + 2[\Delta q_v\times])(\hat{\rho}_{k+1|k} + \Delta\rho) - R(\bar{\mu}_C)R(\bar{q}_{C,k+1})R(q_{O,k+1}) \times$$

$$\times(\hat{r}_{C,k+1|k} + \Delta r_C) - R(\bar{\mu}_C)\rho_C + \xi^r_{k+1} \approx R(\bar{\mu}_C)R(\bar{q}_{C,k+1})R(\hat{q}_{k+1|k})\hat{\rho}_{k+1|k} -$$

$$-R(\bar{\mu}_C)R(\bar{q}_{C,k+1})R(q_{O,k+1})\hat{r}_{C,k+1|k} - R(\bar{\mu}_C)\rho_C -$$

$$-2R(\bar{\mu}_C)R(\bar{q}_{C,k+1})R(\hat{q}_{k+1|k})[\hat{\rho}_{k+1|k}\times]\Delta q_v - R(\bar{\mu}_C)R(\bar{q}_{C,k+1})R(q_{O,k+1})\Delta r_C +$$

$$+R(\bar{\mu}_C)R(\bar{q}_{C,k+1})R(\hat{q}_{k+1|k})\Delta\rho + \xi^r_{k+1} = \hat{r}_{k+1} + G^r_{k+1}\delta x + \xi^r_{k+1}, \qquad (49)$$

where the vector

$$\hat{r}_{k+1} = R(\bar{\mu}_C)[R(\bar{q}_{C,k+1})[R(\hat{q}_{k+1|k})\hat{\rho}_{k+1|k} - R(q_{O,k+1})\hat{r}_{C,k+1|k}] - \rho_C]$$

and 3×21-matrix

$$G^r_{k+1} = (G^{r,\Delta q}_{k+1} : \Theta_{3\times 3} : G^{r,\Delta r}_{k+1} : \Theta_{3\times 6} : G^{r,\Delta\rho}_{k+1} : \Theta_{3\times 3}).$$

In the last expression, the 3×3-matrices have the following form:

$$G^{r,\Delta q}_{k+1} = -2R(\bar{\mu}_C)R(\bar{q}_{C,k+1})R(\hat{q}_{k+1|k})[\hat{\rho}_{k+1|k}\times];$$

$$G^{r,\Delta r}_{k+1} = -R(\bar{\mu}_C)R(\bar{q}_{C,k+1})R(q_{O,k+1});$$

$$G^{r,\Delta\rho}_{k+1} = R(\bar{\mu}_C)R(\bar{q}_{C,k+1})R(\hat{q}_{k+1|k}).$$

An expression (6) for the matrix $R(q)$ and assumption (39) were used to obtain equality (49).

For equation (18) we obtain

$$\breve{\eta}_{k+1} = \bar{\mu}_C \circ \bar{q}_{C,k+1} \circ q_{k+1} \circ \mu_{k+1} + \xi^\eta_{k+1} = \bar{\mu}_C \circ \bar{q}_{C,k+1} \circ \hat{q}_{k+1|k} \circ \Delta q \circ \Delta\mu \circ \hat{\mu}_{k+1|k} +$$

$$+ \xi^\eta_{k+1} = \bar{\mu}_C \circ \bar{q}_{C,k+1} \circ \hat{q}_{k+1|k} \circ \Delta\lambda \circ \hat{\mu}_{k+1|k} + \xi^\eta_{k+1}, \qquad (50)$$

where $\Delta\lambda = \Delta q \circ \Delta\mu$. Using formula (2) for multiplying quaternions, assumption (39) and similar assumptions for $\Delta\mu_0$ and $\Delta\mu_v$, we obtain

$$\Delta\lambda_0 = \Delta q_0 \cdot \Delta\mu_0 - (\Delta q_v, \Delta\mu_v) \approx \Delta q_0 \cdot \Delta\mu_0 \approx 1,$$

$$\Delta\lambda_v = \Delta q_0 \cdot \Delta\mu_v + \Delta\mu_0 \cdot \Delta q_v + \Delta q_v \times \Delta\mu_v \approx \Delta\mu_v + \Delta q_v.$$

ISSN 2786-6491

From here

$$\Delta\lambda = \begin{pmatrix} \Delta\lambda_0 \\ \Delta\lambda_v \end{pmatrix} \approx \begin{pmatrix} 1 \\ \Delta q_v + \Delta\mu_v \end{pmatrix} = \begin{pmatrix} 1 \\ \Theta_{3\times 1} \end{pmatrix} + \begin{pmatrix} 0 \\ \Delta q_v + \Delta\mu_v \end{pmatrix}.$$

Substituting this expression into (50), we get

$$\breve{\eta}_{k+1} \approx \hat{\eta}_{k+1} + Q(\overline{\mu}_C)Q(\overline{q}_{C,k+1})Q(\hat{q}_{k+1|k})\overline{Q}(\hat{\mu}_{k+1|k})\begin{pmatrix} 0 \\ \Delta q_v + \Delta\mu_v \end{pmatrix} + \xi^{\eta}_{k+1} =$$

$$= \hat{\eta}_{k+1} + Q(\overline{\mu}_C)Q(\overline{q}_{C,k+1})Q(\hat{q}_{k+1|k})\overline{Q}_v(\hat{\mu}_{k+1|k})(\Delta q_v + \Delta\mu_v) + \xi^{\eta}_{k+1}, \qquad (51)$$

where quaternion

$$\hat{\eta}_{k+1} = Q(\overline{\mu}_C)Q(\overline{q}_{C,k+1})Q(\hat{q}_{k+1|k})\hat{\mu}_{k+1|k}$$

and 4×3-matrix

$$\overline{Q}_v(\mu) = \begin{pmatrix} -\mu_v^{\mathrm{T}} \\ \mu_0 I_3 - [\mu_v\times] \end{pmatrix}.$$

The equality (51) can be written in the form

$$\breve{\eta}_{k+1} \approx \hat{\eta}_{k+1} + G^{\eta}_{k+1}\delta x + \xi^{\eta}_{k+1}, \qquad (52)$$

where matrices $G^{\eta}_{k+1} = (G^{\eta,\Delta q}_{k+1} : \Theta_{4\times 15} : G^{\eta,\Delta\mu}_{k+1})$, $G^{\eta,\Delta q}_{k+1} = G^{\eta,\Delta\mu}_{k+1} = Q(\overline{\mu}_C)Q(\overline{q}_{C,k+1})\times$ $\times Q(\hat{q}_{k+1|k})\overline{Q}_v(\hat{\mu}_{k+1|k})$.

From expressions (49), (52) and restrictions on measurement noise, we obtain that the components of the increment vector must satisfy the following 7 linear inequalities:

$$\| \breve{r}_{k+1} - \hat{r}_{k+1} - G^{r}_{k+1}\delta x \|_{\infty} \le c^{r}, \qquad (53)$$

$$\| \breve{\eta}_{k+1} - \hat{\eta}_{k+1} - G^{\eta}_{k+1}\delta x \|_{\infty} \le c^{\eta}. \qquad (54)$$

Note that (54) contains 4 inequalities that have to be satisfied using only three variables, namely, a vector $\Delta q_v + \Delta\mu_v$ of dimension 3. In the general case, these inequalities may turn out to be inconsistent, i.e. the solution area may be empty. Therefore, when solving numerically, when finding the intersection with an ellipsoid, three of these four inequalities should be chosen, but in such a way that the discrepancy in the fourth inequality is minimal.

2.3. Problem solution algorithm. We assume that at the moment t_k the estimate $\hat{x}_k$ of the state vector is known, and the parameters of the ellipsoid are also known, the matrix $H_k = H_k^{\mathrm{T}} > 0$. Let us describe the procedure for calculating the estimate $\hat{x}_{k+1}$.

1. We numerically integrate equations (20), (21) and (25) in real time over the interval $[t_k, t_{k+1}]$ under the initial condition $\hat{x}_k$ to calculate estimates $\hat{q}_{k+1|k}$, $\hat{\omega}_{k+1|k}$, $\hat{r}_{C,k+1|k}$ and $\hat{v}_{C,k+1|k}$. For the rest constant components of the state vector, we assume $\hat{l}_{k+1|k} = \hat{l}_k$, $\hat{\rho}_{k+1|k} = \hat{\rho}_k$ and $\hat{\mu}_{k+1|k} = \hat{\mu}_k$.

2. At the moment t_{k+1} we calculate according to expression (48) the matrix A_{k+1} and according to (35) the matrix $H_{k+1|k}$ of the ellipsoid $\delta E_{k+1|k}$.

3. An ellipsoid $\delta E_{k+1}(\delta\hat{x}_{k+1}, H_{k+1})$ is constructed containing the intersection of the ellipsoid $\delta E_{k+1|k}$ and layers corresponding to inequalities (53) and (54) using the algorithm of subsection 2.2. The center of the ellipsoid δE_{k+1}, vector $\delta\hat{x}_{k+1}$ (in the general case $\delta\hat{x}_{k+1} \neq 0$) will satisfy the linearized inequalities (53) and (54).

4. Using the increment vector $\delta\hat{x}_{k+1} = (\Delta\hat{\omega}_{k+1}^{\mathrm{T}}, \Delta\hat{q}_{v,k+1}^{\mathrm{T}}, \Delta\hat{p}_{k+1}^{\mathrm{T}}, \Delta\hat{r}_{T,k+1}^{\mathrm{T}}, \Delta\hat{\rho}_{k+1}^{\mathrm{T}}, \Delta\hat{\mu}_{v,k+1}^{\mathrm{T}})^{\mathrm{T}}$, we calculate the vector

$$\hat{x}_{k+1} = (\hat{\omega}_{k+1}^{\mathrm{T}}, \hat{q}_{k+1}^{\mathrm{T}}, \hat{p}_{k+1}^{\mathrm{T}}, \hat{r}_{T,k+1}^{\mathrm{T}}, \hat{\rho}_{k+1}^{\mathrm{T}}, \hat{\mu}_{k+1}^{\mathrm{T}})^{\mathrm{T}}$$

in accordance with the following formulas:

$$\hat{\omega}_{k+1} = \hat{\omega}_{k+1|k} + \Delta\hat{\omega}_{k+1}, \quad \hat{l}_{k+1} = \hat{l}_{k+1|k} + \Delta\hat{l}_{k+1}, \quad \hat{r}_{C,k+1} = \hat{r}_{C,k+1|k} + \Delta\hat{r}_{C,k+1},$$

$$\hat{v}_{C,k+1} = \hat{v}_{C,k+1|k} + \Delta\hat{v}_{C,k+1}, \quad \hat{\rho}_{k+1} = \hat{\rho}_{k+1|k} + \Delta\hat{\rho}_{k+1}.$$

The quaternion $\hat{q}_{k+1}$ is calculated as follows:

$$\hat{q}_{k+1} = \hat{q}_{k+1|k} \circ \Delta\hat{q}_{k+1} = Q(\hat{q}_{k+1|k})\Delta\hat{q}_{k+1},$$

where $\Delta\hat{q}_{k+1} = (\Delta\hat{q}_{0,k+1}, \Delta\hat{q}_{v,k+1}^{\mathrm{T}})^{\mathrm{T}}$, $\Delta\hat{q}_{0,k+1} = \sqrt{1 - \| \Delta\hat{q}_{v,k+1} \|^2}$. The quaternion $\hat{\mu}_{k+1}$ is calculated similarly:

$$\hat{\mu}_{k+1} = \Delta\hat{\mu}_{k+1} \circ \hat{\mu}_{k+1|k} = \bar{Q}(\hat{\mu}_{k+1|k})\Delta\hat{\mu}_{k+1},$$

where $\Delta\hat{\mu}_{k+1} = (\Delta\hat{\mu}_{0,k+1}, \Delta\hat{\mu}_{v,k+1}^{\mathrm{T}})^{\mathrm{T}}$, $\Delta\hat{\mu}_{0,k+1} = \sqrt{1 - \| \Delta\hat{\mu}_{v,k+1} \|^2}$.

5. For the moment t_{k+1}, we take as the initial ellipsoid $E(0, H_{k+1})$, where H_{k+1} is the matrix of the ellipsoid δE_{k+1}.

The process of estimation will stop when $\delta\hat{x}_{k+1} = 0$, i.e. when the calculated estimates, i.e. the vector $\hat{x}_{k+1|k}$ will satisfy inequalities (19) related to measurements.

The properties of the presented algorithm were studied using numerical simulation.

3. Numerical simulation

Numerical simulation was carried out to test the performance of the proposed algorithms for estimating the parameters of the relative motion of the NSC and the SSC, including influence of the choice of a priori values of the estimated parameters, the quality of the algorithm at different levels of measurement noise. The hovering mode was considered, in which the SSC is at a safe distance from the NSC in the working area of the CVS. The SSC does not perform any maneuvers and carries out measurements of the distance vector and attitude quaternion of the NSC in order to determine the remaining parameters of the relative motion necessary for planning a safe trajectory of approach and capture of the NSC. It is assumed that the SSC is in free orbital flight and is oriented in space in such a way that the NSC is located approximately in the center of the CVS camera frame.

To obtain the «measured values» of the CVS, differential equations (20) and (21) were used, describing the free rotation of the NSC, as well as equation (25) of the relative orbital motion. Various initial values for these equations were considered and ran-

domly selected from a given set of values. In particular, the components $\omega_j(t_0)$, $j=1:3$, of the angular velocity vector $\omega(t_0)$ were chosen randomly from the interval $[-0{,}1, 0{,}1]$ rad/sec. The initial attitude quaternion $q(t_0)$ was chosen in a similar way. Its components $q_j(t_0)$, $j=0:3$, were selected from the interval $[-1, 1]$ and then were normalized. The main moments of inertia of the NSC are $J_1 = 3616$ kgm^2, $J_2 = 7618$ kgm^2, $J_3 = 8098$ kgm^2. The position of the GRF in the TRF was characterized by vector $\rho = (0, 2, 0, 3, 0, 4)^{\mathrm{T}}$ and by nominal known quaternion $\hat{\mu} = (0{,}95, 0{,}16, -0{,}045, 0{,}25)^{\mathrm{T}}$, which value was slightly changed by small unknown increment. The position of the CVS in the CRF was specified by the vector $\rho_C = (1, 2, 0, 4, 0, 0)^{\mathrm{T}}$ and unit quaternion $\mu_C = (1, 0, 0, 0)^{\mathrm{T}}$. Initial position of the SSC c.m. relative to the NSC c.m. was characterized by a vector $r_C = (5, -15, 2)^{\mathrm{T}}$ and a zero vector of relative velocity $v_C(t_0) = (0, 0, 0)^{\mathrm{T}}$ in the ORF. The SSC attitude quaternion $q_C(t)$ was calculated at each time moment from the condition that the NSC was in the center of the CVS frame. These values were used to integrate equations (20), (21) and (25) to calculate the so-called true values of these parameters in time and to form the measured values of distance vector $\breve{r}_k$ and quaternion $\breve{\eta}_k$ in accordance with expressions (17) and (18). Sequences of measurement noise ξ_k^r and ξ_k^{η} were generated as a white noise process, their values are uniformly distributed in intervals $[-c^r, c^r]$ and $[-c^{\eta}, c^{\eta}]$ respectively. The maximum measurement noise values $c^r = 0{,}004$ m and $c^{\eta} = 0{,}003$ were taken from [63], which corresponds to a position accuracy of 4 mm and an attitude within 0,16° in Euler angles. During the simulation, various values of the discrete time period Δ from 0,1 to 1 second, were considered.

The initial values of the estimates for unknown quantities were chosen arbitrarily, including zero, with the exception of estimates for the initial values of $r_C(t_0)$ and $q(t_0)$, which estimates can be obtained using the first measured values of $\breve{r}_0$ and $\breve{\eta}_0$. Various values were considered for the matrix H_0, ranging from $H_0 = 0{,}0001 \cdot I$ and to $H_0 = 4 \cdot I$. The first case corresponded to the situation in which the initial ellipsoid E_0 does not contain the true initial vector. In the case $H_0 = 4 \cdot I$, the ellipsoid E_0 was guaranteed to contain such a vector. During the simulation, it was found that the process of estimating all parameters of relative motion was highly dependent on the choice of the initial approximation and was unstable in most cases. However, with a known or inaccurately known, but given value of the quaternion μ, the estimation algorithm converged for any initial data. Therefore, the simulation results are presented for the case of using a given constant estimate $\breve{\mu} = \Delta\mu \circ \mu$ for the quaternion μ in the estimation algorithm formulas, where the error $\Delta\mu$ was chosen to be small. Plots of changes in time of true values (dashed line) and their estimates (solid line) are presented in Fig. 4–8 for case $H_0 = 0{,}0001 \cdot I$ and $\Delta = 0{,}4$ sec. In Fig. 4 elements of angular velocity ω_k and their estimates $\hat{\omega}_{k,j}$ are shown, plot of change of estimation error $\| \omega_k - \hat{\omega}_k \|_{\infty}$ is presented in Fig. 5.

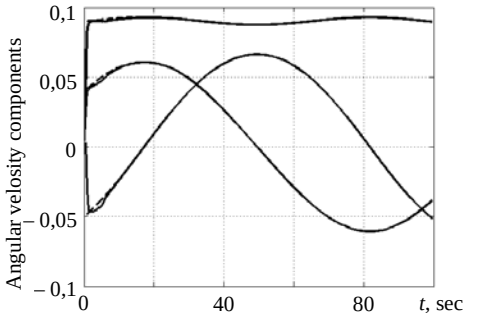

Fig. 4

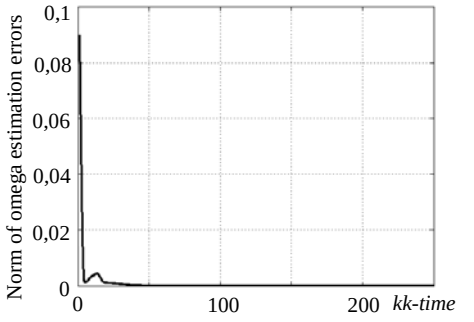

Fig. 5

Similar values for the parameter vector l and its estimate $\hat{l}_k$ are shown in Fig. 6. The plot of change of estimation error $\| l - \hat{l}_k \|_\infty$ is shown in Fig. 7.

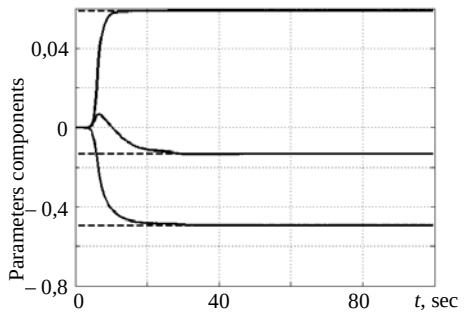

Fig. 6

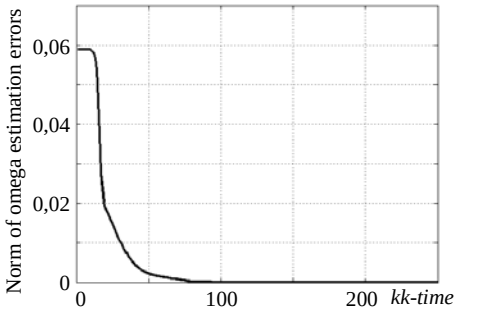

Fig. 7

Components of the vector ρ and its estimate $\hat{\rho}_k$ are presented in Fig. 8.

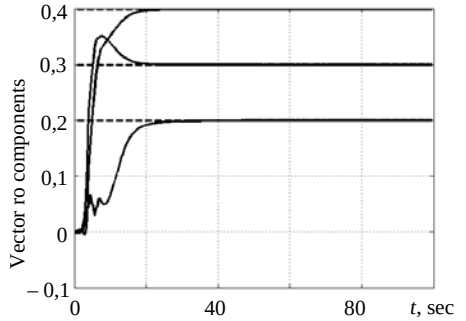

Fig. 8

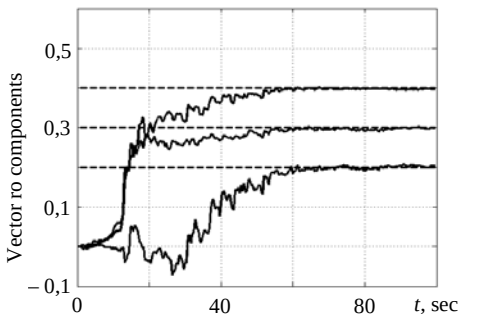

Fig. 9

Fig. 9–11 contain plots of estimates $\hat{\rho}_k$, $\hat{l}_k$ and $\hat{\omega}_k$ for the case of a greater error in measuring the position and attitude of the NSC, namely, for $c^r = 0,02$ m and $c^\eta = 0,06$. These values correspond to the CVS based at the approach [30].

As it can be seen from Fig. 9–11, with a higher intensity of measurement errors the transition process becomes longer and the evaluation plots contain noticeable fluctuations.

ISSN 2786-6491

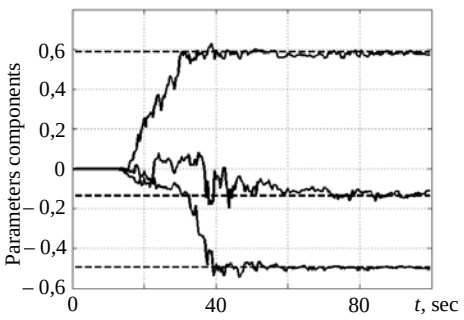

Fig. 10

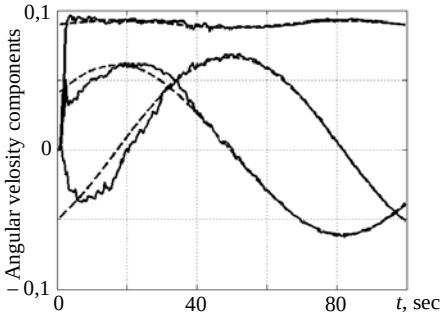

Fig. 11

Conclusion

The need to solve the considered estimation problem is associated with the possibility of implementing safe approach and docking with the NSC, including the case when it is in a state of free rotation. We obtained general functional relation between measured and estimated quantities when the CVS measures the position and attitude of the graphical reference frame relative to the CVS reference frame. An ellipsoidal estimation method is proposed, which does not require knowledge of the stochastic parameters of uncertain quantities, i.e. measurement noise, parameters and initial values of differential equations. Moreover, these quantities are not assumed to be random variables or to have stable stochastic properties.

The results of the numerical simulation showed that the estimation problem under consideration is likely to be ill-conditioned or, in other words, the considered dynamical system for a given set of measurements is close to unobservable. The accuracy of a solution of the simplified estimation problem, in which the quaternion μ is not estimated and instead the algorithm uses some estimate $\breve{\mu}$ of it, degrades as the accuracy of that estimate $\breve{\mu}$ deteriorates. Exact knowledge of μ is crucial to the accuracy of estimation of almost all other quantities. Therefore, it is necessary to ensure an accurate estimation of this value, possibly by involving measurements of additional variables. In the introduction to this work, it is noted that this parameter and other variables can be determined quite accurately, in particular, by introducing coordinates of characteristic points on the NSC surface into the state vector.

The direction of further investigation may be related to further improvement of the estimation algorithm to increase its regularizing properties. It is also of interest to conduct a quantitative comparison of the proposed estimation algorithm, for example, with estimation methods that use various versions of the Kalman filter, namely, to compare the accuracy, convergence speed and computational costs during full scale experiments, i.e. in conditions of real error properties inherent to a particular type of CVS.

М.М. Сальніков, С.В. Мельничук, В.Ф. Губарев

ЕЛІПСОЇДНЕ ОЦІНЮВАННЯ ПАРАМЕТРІВ ОБЕРТАЛЬНОГО ТА ПОСТУПАЛЬНОГО РУХУ НЕКООПЕРАТИВНОГО КОСМІЧНОГО АПАРАТА ЗА ВІЗУАЛЬНОЮ ІНФОРМАЦІЄЮ

Сальніков Микола Миколайович

Інститут космічних досліджень НАН України та ДКА України, м. Київ,

salnikov.nikolai@gmail.com

Мельничук Сергій Вікторович

Інститут космічних досліджень НАН України та ДКА України, м. Київ,

sergvik@ukr.net

Губарев Вячеслав Федорович

Інститут космічних досліджень НАН України та ДКА України, м. Київ,

v.f.gubarev@gmail.com

Використання навколоземного космічного простору в даний час ускладнюється наявністю на орбіті Землі об'єктів космічного сміття, до яких відносяться відпрацьовані ступені ракет-носіїв, недіючі космічні апарати та інші великі і малі об'єкти, пов'язані з діяльністю людини в космосі. Одним з елементів вирішення проблеми космічного сміття є стикування та захоплення некерованого некооперативного космічного об'єкта або космічного апарата так званим орбітальним сервісним космічним апаратом для проведення подальших дій щодо його ремонту, дозаправки або зміни орбіти. Ситуація ускладнюється тим, що під впливом різних факторів некеровані космічні об'єкти знаходяться в стані обертання. Параметри орбітального руху таких об'єктів досить точно відомі з вимірювань із Землі. Для здійснення безпечного зближення і стикування також необхідно знати параметри обертального руху, а також параметри відносного руху. Розглянуто найбільш загальний випадок руху розташованого на еліптичній орбіті некооперативного космічного апарата, який знаходиться у стані вільного обертання. Передбачається, що тривимірна графічна модель такого корабля відома. Сервісний космічний апарат (СКА) оснащено монокамерою, яка робить знімки некооперативного космічного апарата (НКА). На основі порівняння характерних особливостей фотографій та зображень, що отримуються за допомогою графічної моделі, система комп'ютерного зору (СКЗ) визначає вектор відстані до так званої графічної системи координат, жорстко закріпленої на НКА, та кватерніон її відносної орієнтації. Конкретний тип СКЗ не розглядається. Передбачається, що СКА може здійснювати маневри поблизу НКА. Усі параметри кутового руху СКА вважаються відомими. У даній роботі розглядається найбільш загальний випадок відносного руху СКА і НКА. За допомогою кватерніонного числення отримано всі основні кінематичні та динамічні рівняння. Параметрів, що вимірюються, недостатньо для безпечного зближення та стикування з НКА. Стохастичні характеристики похибок вимірювання СКЗ не вважаються відомими і, відповідно, не використовуються. Для похибок вказані лише їх максимальні значення. Розглядається новий динамічний множинний фільтр з використанням еліпсоїдів для вирішення задачі визначення параметрів відносного руху НКА, що перебуває у вільному некерованому русі. Фільтр можна реалізувати в умовах обмежених обчислювальних можливостей, доступних на бортових процесорах. До параметрів відносного руху відносяться вектор відстані між центрами маси (ц.м.) НКА і СКА, вектор відносної швидкості, кватерніон орієнтації головних осей інерції НКА відносно інерційної системи координат, відношення моментів інерції НКА, вектор положення ц.м. НКА в графічній системі координат. Властивості запропонованого алгоритму продемонстровано за допомогою чисельного моделювання. Отримані результати планується використати при розробці, створенні та випробуванні навігаційної системи зближення та стикування СКА, який розробляється групою підприємств космічної галузі України під керівництвом ТОВ «Курс-орбітал» (https://kursorbital.com/).

Ключові слова: відносні параметри руху, космічний апарат, оцінювання, відеозображення.

REFERENCES

1. Moghaddam B.M., Chhabra R. On the guidance, navigation and control of in-orbit space robotic missions: a survey and prospective vision. *Acta Astronautica*. 2021. Vol. 184. P. 70–100. DOI: https://doi.org/10.1016/j.actaastro.2021.03.029

2. Fokov A.A. Analysis of the state of the art in the problem of determining the pose of on-orbit service objects. *Technical mechanics*. 2023. N 1. C. 54–67 (in Ukrainian).
3. Opromolla R., Fasano G., Rufino G., Grassi M. A review of cooperative and uncooperative spacecraft pose determination techniques for close-proximity operations. *Progress in Aerospace Sciences.* 2017. Vol. 93. P. 53–72. DOI: https://doi.org/10.1016/j.paerosci.2017.07.001
4. Pasqualetto Cassinis L., Fonod R., Gill E. Review of the robustness and applicability of monocular pose estimation systems for relative navigation with an uncooperative spacecraft. *Progress in Aerospace Sciences.* 2019. Vol. 110. P. 100548. DOI: https://doi.org/10.1016/j.paerosci.2019.05.008
5. Bragazin A.F. Control of spacecraft rendezvous (navigation, guidance, motion correction). Korolev : RSC «Energia», 2018. 470 p. (in Russian).
6. Farrell J.A. Aided navigation. GPS with high rate sensors. New York : The McGraw-Hill Companies, 2008. 553 p.
7. Fehse W. Automated rendezvous and docking of spacecraft. Cambridge : Cambridge University Press, 2003. 517 p.
8. Aghili F. Automated rendezvous & docking without impact using a reliable 3D vision system. *Guidance, Navigation, and Control Conference.* Canada : Toronto; Ontario. 2010. 2–5 August. DOI: https://doi.org/10.2514/6.2010-7602
9. Opromolla R., Nocerino A. Uncooperative spacecraft relative navigation with LIDAR-based unscented Kalman filter. *IEEE Access.* 2019. Vol. 7. P. 180012–180026. DOI: https://doi.org/10.1109/ACCESS.2019.2959438
10. Nocerino A., Opromolla R., Fasano G., Grassi M. LIDAR-based multi-step approach for relative state and inertia parameters determination of an uncooperative target. *Acta Astronautica*. 2021. Vol. 181. P. 662–678. DOI: https://doi.org/10.1016/j.actaastro.2021.02.019
11. Aghili F., Kuryllo M., Okouneva G., English Ch. Fault-tolerant position/attitude estimation of free-floating space objects using a laser range sensor. *IEEE Sensors Journal.* 2011. Vol. 11, N 1. P. 176–185. DOI: https://doi.org/ 10.1109/JSEN.2010.2056365
12. Aghili F., Su C. Robust relative navigation by integration of ICP and adaptive Kalman filter using laser scanner and IMU. *IEEE/ASME Transactions on Mechatronics*. 2016. Vol. 21, N 4. P. 2015–2026. DOI: https://doi.org/10.1109/TMECH.2016.2547905
13. Kelsey J.M., Byrne J., Cosgrove M., Seereeram S., Mehra R.K. Vision-based relative pose estimation for autonomous rendezvous and docking. *IEEE Aerospace Conference*. 2006. P. 20–39. DOI: https://doi.org/10.1109/AERO.2006.1655916
14. Segal S., Carmi A., Gurfil P. Vision-based relative state estimation of non-cooperative spacecraft under modeling uncertainty. NJ : IEEE Publ. *Aerospace Conference. Piscataway*. 2011. P. 1–8. DOI: https://doi.org/10.1109/AERO.2011.5747479
15. Oumer N.W., Panin G. Tracking and pose estimation of non-cooperative satellite for on-orbit servicing. Italy : Turin. *Proseedings of the conference i-SAIRAS(ESA).* 2012. 4-6 Sep.
16. D'Amico S., Benn M., Jørgensen J.L. Pose estimation of an uncooperative spacecraft from actual space imagery. *International Journal of Space Science and Engineering.* 2014. Vol. 2, N 2. P. 171–189. DOI: https://doi.org/ 10.1504/IJSPACESE.2014.060600
17. Yu X., Yu F., He Z. Stereo vision based relative state estimation for non-cooperative spacecraft with outliers. *Proceedings of the 33rd Chinese Control Conference*. 2014. P. 763–769. DOI: https://doi.org/ 10.1109/ChiCC.2014.6896723
18. Volpe R., Sabatini M., Palmerini G.B. Pose and shape reconstruction of a noncooperative spacecraft using camera and range measurements. *International Journal of Aerospace Engineering*. 2017. Vol. 2017, article ID 4535316. 13 p. DOI: https://doi.org/10.1155/2017/4535316
19. Dementhon D.F., Davis L.S. Model-based object pose in 25 lines of code. *International Journal of Computer Vision.* 1995. Vol. 15. P. 123–141. DOI: https://doi.org/10.1007/BF01450852
20. Masutani Y., Iwatsu T., Miyazaki F. Motion estimation of unknown rigid body under no external forces and moments. *Proceedings of the 1994 IEEE International Conference on Robotics and Automation.* 1994. Vol. 2. P. 1066–1072. DOI: https://doi.org/ 10.1109/ROBOT.1994.351227
21. Zhang Shijie, Liu Fenghua, Cao Xibin, He Liang. Monocular vision-based two-stage iterative algorithm for relative position and attitude estimation of docking spacecraft. *Chinese Journal of Aeronautics.* 2010. Vol. 23, N 2. P. 204–210. DOI: https://doi.org/10.1016/S1000-9361(09)60206-5
22. Capuano V., Kim K., Harvard A., Soon-Jo Chung. Monocular-based pose determination of uncooperative space objects. *Acta Astronautica*. 2020. Vol. 166. P. 493–506. DOI: https://doi.org/10.1016/j.actaastro.2019.09.027

23. Espinoza A.T., Setterfield T.P. Point-to-CAD 3D registration algorithm for relative navigation using depth-based maps. *2019 IEEE Aerospace Conference*. 2019. P. 1–7. DOI: https://doi.org/10.1109/AERO.2019.8742148
24. Liang H., Wang J., Wang Y., Huo W. Monocular-vision-based spacecraft relative state estimation under dual number algebra. *Proceedings of the Institution of Mechanical Engineers, Part G: Journal of Aerospace Engineering.* 2020. Vol. 234. P. 221–235. DOI: https://doi.org/10.1177/0954410019864754
25. Ivanov D., Ovchinnikov M., Sakovich M. Relative pose and inertia determination of unknown satellite using monocular vision. *International Journal of Aerospace Engineering*. 2018. Vol. 2018, article ID 9731512. DOI: https://doi.org/10.1155/2018/9731512
26. Salnikov N.N., Melnychuk S.V., Gubarev V.F. Ellipsoidal pose estimation of an uncooperative spacecraft from video image data. *Control Systems: Theory and Applications. River Publishers Series in Automation, Control and Robotics*. 2018. P. 169–195.
27. Grishin V.A., Zhukov B.S. Features of the problem of pattern recognition in relation to problems of relative navigation during docking of spacecraft. *Modern problems of Earth remote sensing from space.* 2020. Vol. 17, N 7. P. 58–66 (in Russian).
28. Molina Saqui J.C., Tkachev S.S. Kalman filter application for the angular motion estimation by video processing. *Preprints of the Keldysh Institute of Applied Mathematics*. 2021. N 27. 27 p. DOI: https://doi.org/10.20948/prepr-2021-27-e
29. Shi J.-F., Ulrich S., Ruel S. Spacecraft pose estimation using principal component analysis and a monocular camera. *AIAA Guidance, Navigation, and Control Conference*. 2017. Grapevine, Texas, 9–13 January 2017. P. 1034. DOI: https://doi.org/10.2514/6.2017-1034
30. Gubarev V., Salnikov N., Melnychuk S., Shevchenko V., Maksymyuk L. Special cases in determining the spacecraft position and attitude using computer vision system. *Advanced Control Systems: Theory and Applications. River Publishers Series in Automation, Control and Robotics*. 2021. P. 289–316.
31. Koshkin N., Melikyants S., Korobeinikova E., Shakun L., Strakhova S., Kashuba V., Romanyuk Ya., Terpan S. Simulation of the orbiting spacecraft to analysis and understand their rotation based on photometry. *Odessa Astronomical Publications*. 2019. Vol. 32. P. 158–161. DOI: https://doi.org/10.18524/1810-4215.2019.32.183899
32. Markley F.L., Crassidis J.L. Fundamentals of spacecraft attitude determination and control. New York : Springer Science+Business Media, 2014. 495 p.
33. Rauschenbakh B.V., Tokar E.N. Spacecraft orientation control. Moscow : Nauka, 1974. 600 p. (in Russian).
34. Aghili F. A Prediction and motion-planning scheme for visually guided robotic capturing of free-floating tumbling objects with uncertain dynamics. *IEEE Transactions on Robotics*. 2012. Vol. 28, N 3. P. 634–649. DOI: https://doi.org/10.1109/TRO.2011.2179581
35. Aghili F., Parsa K. Motion and parameter estimation of space objects using laser-vision data. *Journal of Guidance, Control, and Dynamics*. 2009. Vol. 32, N 2. P. 537–549. DOI: https://doi.org/10.2514/1.37129
36. Stainfeld D., Rock S.M. Rigid body inertia estimation with applications to the capture of a tumbling satellite. GA : Savannah. *Proceedings of 19th AAS/AIAA Spaceflight Mechanics Meeting.* 2009. P. 343–356.
37. Kalman filtering and neural networks (edited by S. Haykin). New York; Toronto : John Wiley&Sons, Inc., 2001. 284 p.
38. Arulampalam M. S., Maskell S., Gordon N., Clapp T. A tutorial on particle filters for online nonlinear/non-Gaussian bayesian tracking. *IEEE Transactions on Signal processing*. 2002. Vol. 50, N 2. P. 174–188. DOI: https://doi.org/10.1109/78.978374
39. Cheng Y., Crassidis J.L. Particle filtering for attitude estimation using a minimal local-error representation. *Journal of Guidance, Control, and Dynamics*. 2010. Vol. 33, N 4. P. 1305–1310. DOI: https://doi.org/10.2514/1.47236
40. Schweppe F.C. Uncertain dynamic systems. Englewood Cliffs. NJ : Prentice-Hall, 1973. 563 p.
41. Kuntzevich V.M., Lychak M. Guaranteed estimates, adaptation and robustness in control systems. Berlin; New York : Springer-Verlag, 1981. 211 p.
42. Chernousko F. L. State estimation for dynamic systems. Boca Raton : CRC Press, 1994. 394 p.
43. Kurzhanski A.B., Valyi I. Ellipsoidal calculus for estimation and control. Boston : Birkhauser, 1997. 336 p.
44. Chabane S.B., Maniu C. S., Alamo T., Camacho E.F., Dumur D. A new approach for guaranteed ellipsoidal state estimation. *IFAC Proceedings Volumes*. 2014. Vol. 47, N 3. P. 6533–6538. DOI: https://doi.org/10.3182/20140824-6-ZA-1003.01629

45. Blanchini F., Miani S. Set-theoretic methods in control. Switzerland : Springer International Publishing, 2015. 640 p.
46. Poznyak A., Polyakov A., Azhmyakov V. Attractive ellipsoids in robust control. Switzerland : Springer International Publishing, 2014. 365 p.
47. Scholte E., Campbell M.E. A nonlinear set-membership filter for on-line applications. *Int. J. Robust Nonlinear Control.* 2003. Vol. 13. P. 1337–1358. DOI: https://doi.org/10.1002/rnc.856
48. Zhou B., Qian K., Ma X.-D., Dai X.-Zh. A new nonlinear set membership filter based on guaranteed bounding ellipsoid algorithm. *Acta Automatica Sinica*. 2013. Vol. 39, N 2. P. 146–154. DOI: https://doi.org/10.1016/S1874-1029(13)60017-8
49. Wang Z., Shen X., Zhu Y., Pan. J. A tighter set-membership filter for some nonlinear dynamic systems. *IEEE Access*. 2018. Vol. 6. P. 25351–25362. DOI: https://doi.org/ 10.1109/ACCESS. 2018.2830350
50. Wang Z., Shen X., Liu H., Meng F., Zhu Y. Dual set membership filter with minimizing nonlinear transformation of ellipsoid. *IEEE Transactions on Automatic Control*. 2022. Vol. 67, N 5. P. 2405–2418. DOI: https://doi.org/10.1109/TAC.2021.3081078
51. Massioni P., Salnikov N., Scorletti G. Ellipsoidal state estimation based on sum of squares for non-linear systems with unknown but bounded noise. *IET Control Theory&Applications*. 2019. Vol. 13, N 12. P. 1955–1961. DOI: https://doi.org/10.1049/iet-cta.2018.5072
52. Volosov V.V., Tyutyunnik L.I. Development and analysis of robust algorithms for guaranteed ellipsoidal estimation of the state of multidimensional linear discrete dynamic systems. Part I. *Journal of Automation and Information Sciences*. 2000. Vol. 32, N 3. P. 37–46. DOI: https://doi.org/ 10.1615/JAutomatInfScien.v32.i3.50
53. Volosov V.V., Tyutyunnik L.I. Development and analysis of robust algorithms for guaranteed ellipsoidal estimation of the state of multidimensional linear discrete dynamic systems. Part 2. *Journal of Automation and Information Sciences*. 2000. Vol. 32, N 11. P. 13–23. DOI: https://doi.org/ 10.1615/JAutomatInfScien.v32.i11.20
54. Salnikov N.N. On one modification of linear regression estimation algorithm using ellipsoids. *Journal of Automation and Information Sciences*. 2012. Vol. 44, N 3. P. 15–32. DOI: https://doi.org/ 10.1615/JAutomatInfScien.v44.i3.20
55. Salnikov N.N. Estimation of state and parameters of dynamic system with the use of ellipsoids at the lack of a priori information on estimated quantities. *Journal of Automation and Information Sciences*. 2014. Vol. 46, N 4. P. 60–75. DOI: https://doi.org/ 10.1615/JAutomatInfScien.v46.i4.50
56. Markley F.L. Multiplicative versus additive filtering for spacecraft attitude determination. 2003. https://ntrs.nasa.gov/citations/20040037784
57. Crassidis J.L., Markley F.L., Cheng Y. Survey of nonlinear attitude estimation methods. *Journal of Guidance, Control and Dynamics*. 2007. Vol. 30, N 1. P. 12–28. DOI: https://doi.org/ 10.2514/1.22452
58. Salnikov N.N., Melnychuk S.V., Gubarev V.F., Maksymyuk L.V., Shevchenko V.M. Relative motion parameters estimation of a non-cooperative spacecraft from visual information. *Space Science and Technology*. 2023. Vol. 29, N 3. P. 16–33. DOI: https://doi.org/10.15407/knit2023. 03.016
59. Schaub H., Junkins J.L. Analytical Mechanics of Space Systems. 2009. Reston : AIAA, 827 p.
60. Amelkin N.I. Rigid body dynamics. Moscow : MIPT, 2012. 80 p. https://studylib.ru/doc/ 1678659/n.i.-amel._kin-dinamika-tverdogo-tela (in Russian).
61. Mirer S.A. Mechanics of space flight. Orbital motion. 2013. (electronic edition of the Keldysh Institute of Applied Mathematics. https://www.keldysh.ru/microsatellites/Space_flight_mechanics_ part_1.pdf (in Russian).
62. Pontryagin L.S. Ordinary differential equations. Moscow : Nauka, 1982. 332 p. (in Russian).
63. Liu G., Xu C., Zhu Y., Zhao J. Monocular vision-based pose determination in close proximity for low impact docking. *Sensors*. 2019. Vol. 19, N 15. P. 1–17. DOI: https://doi.org/10.3390/ s19153261

Submitted 20.11.2023